ASTRONOMY & ASTROPHYSICS
SUPPLEMENT SERIES

Astron. Astrophys. Suppl. Ser. **88**, 133-153 (1991)

Photometric and spectroscopic observations of the cluster of galaxies Abell 2390*

J.-F. Le Borgne[1], G. Mathez[1], Y. Mellier[1], R. Pelló[2], B. Sanahuja[2] and G. Soucail[1]

[1] Observatoire Midi-Pyrénées, 14 Av. Edouard Belin, 31400 Toulouse, France
[2] Departament de Física de la Atmosfera, Astronomia i Astrofísica, Universitat de Barcelona, and Grup d'Astrofísica del IEC, Av. Diagonal, 647, 08028 Barcelona, Spain

Received April 11; accepted October 24, 1990

Abstract. — We present spectroscopic and photometric observations in a $6' \times 6'$ field centered on the rich cluster of galaxies Abell 2390. The photometry concerns 700 objects and the spectroscopy 72 objects. Our redshift survey shows that the mean redshift of the cluster is 0.232. An original method for automatic determination of the spectral type of galaxies is presented.

Key words: Clusters of galaxies — redshifts of galaxies.

1. Introduction.

Abell 2390 is a cluster of distance class 6 and richness class 1 (Abell *et al.* 1989) dominated by a giant elliptical galaxy which shows all characteristics of a cD galaxy. This cluster is of great interest because of the presence of a "straight" arc and of numerous "arclets" which could be gravitationally distorted images (Mellier 1989). The straight arc has been spectroscopically identified as a lensed background galaxy at a redshift of 0.913 (Pelló *et al.* 1989, 1991). As most of the clusters where arcs are observed, A2390 is a strong X-ray emitter. Its total X-ray luminosity is 9.77×10^{44} ergs s^{-1} in the range 2-6 keV (H_0= 75 km s^{-1} Mpc^{-1}) (Kowalski *et al.* 1984) and 4.67×10^{44} ergs s^{-1} in the range 0.7–3.5 keV (Ulmer *et al.* 1986). Ulmer *et al.* (1986) and McMillan *et al.* (1989) have published X-ray maps from the Einstein Observatory observations. Owen *et al.* (1982) have detected a radio source at 1400 MHz close to the central galaxy (0.35 ± 0.09 J_y).

In a first paper (Pelló *et al.* 1991), we study the straight arc and the arclets. The detailed analysis of the cluster will be given in a forthcoming paper (Mellier *et al.* 1991). The analysis of the central emission-line cD galaxy and of the other emission-line galaxies in the cluster will be published in Soucail *et al.* (1991).

In the present paper we give the catalogue of the photometric and spectroscopic data of objects in the field of A2390.

2. Observations.

Photometric observations were performed during 2 runs at the 2.5 m Isaac Newton Telescope and 3.6 m Canada-France-Hawaii Telescope. Spectroscopic data were obtained during 5 runs at the 4.2 m William Herschel Telescope, the CFHT and the 3.6 m ESO telescope. The spectroscopic runs were mainly dedicated to long exposure time spectra of the faint giant arc for which we have accumulated 15 one-hour spectra with the WHT. However, time was reserved to get spectra of other galaxies, in addition to the faint ones that we obtained on the same CCD frame as the arc.

Sky coordinates of the cluster may be found in Abell *et al.* (1989) or in Owen *et al.* (1982) but with a precision of the order of 1′ only. We have computed the coordinates of the central galaxy with a better precision ($\approx 2''$) by measuring its position relative to neighboring SAO stars on prints of the Palomar Sky Survey: α_{1950} = 21h 51mn 14.3s ; δ_{1950} = 17° 27′ 34.9″.

2.1. Photometry.

Both photometric runs used RCA2 CCD's with pixel sizes of 0.74″ for the INT and 0.205″ for the CFHT on good photometric conditions. Details about the frames are given in Table 1. The frames from INT ($4.0' \times 6.3'$) were obtained with a Johnson B filter (hereafter noted B_j) and Thuan-Gunn g

Send offprint requests to: J.-F. Le Borgne.

* Based on observations made with the William Herschel and Isaac Newton Telescopes operated on the island of La Palma by the Royal Greenwich Observatory in the spanish Observatorio del Roque de los Muchachos of the Instituto de Astrofisica de Canarias, the Canada-France-Hawaii Telescope, and the 3.6m telescope at the European Southern Observatory (La Silla, Chile).

and r filters. A second set of B_j and r frames were rotated by 90° relative to the first one, in order to cover almost completely a field of 6.3′ × 6.3′ for filters B_j and r. The CFHT frames used Bessel B and R filters (hereafter noted B_b and R_b). They only concern the central part of the cluster on a field of 3.5′ × 2.2′ but with fainter limiting magnitudes and better spatial resolution thanks to a better seeing and smaller pixel size. Both B_b and R_b CFHT frames are the sum of 3 frames with individual exposure times of 30mn and 15mn respectively.

The photometric calibration was done using Johnson and Thuan-Gunn system standard stars from Kent (1985) and Thuan & Gunn (1976), and standard stars in the globular cluster M92 (Kent 1985, for g and r; Sandage & Walker 1966, for B_j). Bessel standard stars in the globular cluster NGC 7006 were taken from Christian *et al.* (1985). The 2 frames obtained with the r filter at INT are shown in Figures 1 and 2.

TABLE 1. *Characteristic of the photometric frames.*

date	telescope	filter	seeing	mag. of completeness	exposure time
19 JUL 88	INT	B_j	1.0"	23.7	45 mn
19 JUL 88	INT	g	1.0"	23.2	35 mn
19 JUL 88	INT	r	1.0"	22.3	30 mn
20 JUL 88	INT	B_j	1.3"	23.7	45 mn
20 JUL 88	INT	r	1.3"	22.3	30 mn
12-13 AUG 88	CFHT	B_b	0.7"	24.4	3 x 30 mn
12-13 AUG 88	CFHT	R_b	0.7"	23.0	3 x 15 mn

2.2. SPECTROSCOPY.

ESO (1988) and WHT runs used a long slit, with respectively EFOSC1 and FOS, while CFHT and ESO (1989) runs used the MOS system PUMA (Fort *et al.* 1986). Table 2 gives the characteristics of the spectroscopic runs. The exposure times were: 4h09mn at CFHT in September 1988, 2h at ESO in October 1988, 2h at CFHT in June 1989, and 1h50mn at ESO in September 1989. The exposure times for the WHT range from 30mn to 1 hour and some spectra are the result of the sum of several exposures. Since we used long slits, most objects were not well centered on the slit, and consequently the quality of the spectra is not always related to the magnitude of the objects. WHT spectra were calibrated with the standard star G138-31 (Filippenko & Greenstein 1984), ESO spectra with Feige 24 (Oke 1974) for October 1988 run and Feige 110 (Stones 1977) for September 1989 run: we only give fluxes in arbitrary units. Figure 3 shows some representative F_λ spectra from the WHT and from ESO. CFHT spectra are not displayed because they were not flux calibrated due to the absence of calibration stars (technical problems for the first run and bad weather conditions for the second run). However, redshifts can be determined from CFHT spectra. Some objects are common to several runs and allow comparison of redshifts: the agreement between them is within the measurement errors, with the exception of the first CFHT run where a systematic shift of 0.002 was observed.

3. The photometric catalogue.

Table 3 gives the magnitudes and colour indices of the 697 objects detected on both INT and CFHT frames. From left to right, the columns of Table 3 are:

Column 1: identification number.

Column 2: x position in arc seconds relative to the central galaxy, increasing westward.

Column 3: y position in arc seconds relative to the central galaxy, increasing northward.

Column 4: B_j magnitude (isophotal mag. 27.0).

Column 5: g magnitude (isophotal mag. 26.5).

Column 6: r magnitude (isophotal mag. 26.0).

Column 7: B_j-g (isophotal mag. g 25.5).

Column 8: g-r (isophotoal mag. g 25.5).

Column 9: B_j-r (isophotal mag. B_j 26.5).

Column 10: B_b magnitude (isophotal mag. 26.5).

Column 11: R_b magnitude (isophotal mag. 25.0).

Column 12: B_b-R_b (isophotal mag. B_b 26.5).

When a magnitude is noted "n.d.", it means that the object is not detected in the corresponding frame. When nothing is printed, the object is outside the concerned CCD

TABLE 2. *Spectroscopic runs.*

date site	CCD	pixel size	slit or hole size	wavelength range (Å)	dispersion (Å/pix.)	spectral resol. (Å)	number of objects
SEP 88 CFHT	Thomson 576x384	0.41"	2.1" holes	4500-7000	3.7	11.1	17
OCT 88 ESO	RCA bin. 1024x640	0.67"	1.5"x3.6'	4000-7000	6.1	18.3	1
JUN 89 CFHT	Ford 512x512	0.41"	2.1" holes	4500-7500	6.7	20.1	9
AUG 89 WHT	GEC 578x384	0.67"	2" x 3'	4900-9000	8.7	22.3	61
SEP 89 ESO	RCA bin. 1024x640	0.67"	1.5"x3.6'	4000-7000	6.1	18.3	13

frame. For the colour indices, both magnitudes are measured inside the same elliptical contour corresponding to the isophotal magnitude of the reference filter (see above columns 7, 8 and 12). The reason for this is that it is important to calculate the colour indices by measuring the intensity in the same physical area for both filters, otherwise the colour indices would be meaningless. When no colour is given it means either that the object is not detected in one or two frames, or that the magnitude for a filter inside the reference filter isophotal contour is too large. In Figures 4 and 5, one can find identification charts of the field. Only the brightest objects are numbered in Figure 4 to avoid confusion.

The photometry was performed with the "Amaphot" software package developed at the Toulouse Observatory. The internal accuracy of the INT photometry is about 0.05 magnitude in B_j and g for all the objects. In the case of r, the internal errors are less than 0.03 up to magnitude 20, 0.04 for $20 < r < 22$, and 0.05 for $r > 22$. The estimated internal errors of the CFHT photometry are: 0.02 mag. for $B_b < 23$ and $R_b < 22$, 0.04 mag. in the ranges $23 < B_b < 24$ and $22 < R_b < 23$, and 0.07 mag. for $B_b > 24$ and $R_b > 23$. All these errors are estimated by comparing magnitudes obtained for the same objects in different frames when possible.

Although they concern the same parts of the spectrum, B_j and B_b magnitudes on the one hand, r and R_b magnitudes on the other hand, are not in principle comparable. Indeed we find a systematic difference of about 0.5 magnitude between B_b and B_j, However no difference is found between r and R_b on the average. Furthermore, the difference of spectral response of the filters leads to a dispersion which is not due to a photometric error.

4. The spectroscopic catalogue.

Table 4 gives the redshifts of the galaxies measured on WHT, ESO or CFHT spectra. From left to right, the columns of Table 4 are:

Column 1: identification number.

Column 2: redshift.

Column 3: r magnitude from Table 3.

Column 4: B_j-r from Table 3.

Column 5: radial velocity relative to the cluster centre of mass for cluster members.

Column 6: spectral type of the galaxy determined visually.

Column 7: signal to noise ratio.

Column 8: χ^2_{min} (see below).

Column 9: spectral type of the galaxy determined "automatically".

Column 10: telescopes where the spectra were obtained.

Column 11: list of detected lines.

The objects for which a spectrum is given in Tables 4 and 5 can be identified in Figures 4 and 5. Object # 698 whose spectrum was obtained at ESO is outside the INT field: Figure 6 allows to identify this galaxy.

The redshifts were determined by visual identification of lines. Since the spectral resolution is low, of the order of 20Å FWHM, one cannot determine the wavelength of the lines with a precision better than $\approx$ 1 pixel, which roughly corresponds to 8 Å/6000 Å $\simeq$ 0.0013 for the uncertainty on a redshift based on a single line. Indeed, we find that the mean value of the standard deviations on our redshift measurements is 0.0014. The redshift uncertainties given in table 4 are equal to this average standard deviation divided by the square root of number of used lines. It corresponds to uncertainties on radial velocity ranging from 120 to 420 km s^{-1}.

The spectral types of the galaxies are determined by fitting redshifted non-evolved synthetic spectra (Rocca-Volmerange & Guiderdoni 1988) on the observed spectra by 2 ways. First, the spectral type was determined visually from the best fit to the synthetic spectra (see Tab. 4). In a second step, we tried to find the best spectral type(s) automatically. The aim of this last method is to give an estimation of the spectral type (for a given library of synthetic spectra) for a large sample of galaxies and to give a warning to the user for peculiar spectra to be visually examined. For this, we choose a spectral range as extended as possible where the signal is not too noisy (outside sky emission line residuals) and where we compute a standard deviation σ and a signal to noise ratio S/N :

$$\sigma^2 = \frac{\sum (S_{obs} - S_{smooth})^2}{n-1} \qquad S/N = \frac{\overline{S_{obs}}}{\sigma}$$

S_{obs} is the observed spectrum whose mean value is $\overline{S_{obs}}$; S_{smooth} is a strong smoothing of the observed spectrum; value greater than 3σ are excluded in a second iteration to compute σ.

On the other hand, a reduced χ^2 value is computed by adding the square of the difference between the observed spectrum and the synthetic spectra normalised to the observed spectrum:

$$\chi^2 = \frac{\sum (S_{obs} - S_{synthe})^2}{(n-2)\,\sigma^2}$$

$\chi^2$is computed for the 6 spectral types E, Sa, Sb, Sc, Sd and Im as defined by Rocca-Volmerange & Guiderdoni (1988). The best fit among the 6 spectral types is obtained for χ^2 minimum (χ^2_{min}) and the goodness of the fit is characterized by $\chi^2_{min} \approx 1$.

To estimate to what extent a given value of χ^2_{min} may be considered as a good fit we must evaluate the noises intervening in the computation of χ^2 :

σ^2 is the sum of the CCD read-out noise and the photon

noise.
σ_e^2 being an error due to the differences between the library spectra and the observed spectrum and to flux calibration errors, then:

$$\chi^2 \simeq \frac{\sigma^2 + \sigma_e^2}{\sigma^2} = 1 + \frac{\sigma_e^2}{\sigma^2}$$

When S/N is small, we may expect that the fluctuations of the signal σ^2 are much larger than the difference between the observed spectrum and any synthetic spectrum and then that $\chi^2 \approx 1$ for all spectral types. Our experience shows that it is difficult to find a good fit for $S/N < 5$. When S/N is large (small σ), we may have $\chi^2 \approx 1$ if $\sigma_e^2 \ll \sigma^2$ (good fit) or $\chi^2 = \infty$ if $\sigma_e^2 \gg \sigma^2$ (poor fit). $\chi^2_{\min}$ may be much greater than 1 when the observed spectrum shows emission lines or when it is much redder than an E galaxy or much bluer than an Im galaxy.

We consider a good fit when $\sigma_e^2 \leq \sigma^2$: we then say that spectral types are possible ones for $\chi^2 \leq 2$. In Table 4, these spectral types are given in column 9: for example, E/Sb means that E, Sa and Sb types are possible. Column 8 gives $\chi^2_{\min}$ computed as the mean of the values of χ^2 for the synthetic spectra with $\chi^2 \leq 2$. When $S/N < 5$, a "?" is added to the list of possible spectral types which are given only if their number is less than 4. When $\chi^2 > 2$, a "!" is added.

In our sample, the WHT spectra were fitted on the range 5000-8000 Å and the ESO spectra on the range 4500-6000 Å. $\chi^2_{\min}$ ranges from 1 to 10.6 and the agreement between the determinations by the 2 methods is usually good.

Table 5 gives the list of objects identified as stars from their spectra: r and B_j-r from Table 3 are also given for these stars.

The mean spectroscopic redshift of the cluster is 0.232 ± 0.012 while the estimated photometric one is 0.195 (Kowalski *et al.* 1984). As can be seen in Table 4, A2390 contains an unusual number of emission-line galaxies. In particular, the radio emitting central galaxy exhibits strong emission lines. Emission lines are found in 11% of the A2390 galaxies in the present sample. This is one of the largest proportions of emission-line galaxies known in a cluster: as noted by Dressler *et al.* (1985), 7% of nearby cluster galaxies show emission lines while this ratio is 31% for field galaxies. The expression given by Danese *et al.* (1980) is used to compute individual radial velocities for the 43 good signal to noise spectra of cluster members. This leads to a velocity dispersion of 2112 km s^{-1} (+274 −197 km s^{-1} at 68% confidence level). This is a high value for a cluster of galaxies. The histogram of the radial velocities shows that this dispersion is not due to a bimodal velocity distribution. The distribution has a single peak but has more galaxies with a high relative velocity than a normal distribution. This is explained by a velocity gradient we found in this cluster which will be discussed elsewhere.

Acknowledgements.

The authors wish to thank M. Breare for his support during observations with the WHT at La Palma, M. Cailloux who took part in ESO observations and data reduction and CFHT data reduction, B. Fort for his useful suggestions, B. Rocca-Volmerange and B. Guiderdoni to allow the use of their synthetic spectra.

References

Abell G.O., Corwin H.G. and Olowin R.P. 1989, ApJS 70, 1
Christian C.A., Adams M., Barnes J.V., Butcher H., Hayes D.S., Mould J.R. and Siegel M. 1985, PASP 97, 363
Danese L., De Zotti G., di Tullio G. 1980, A & A 82, 322
Dressler A., Thompson I.B., Shectman S.A. 1985, ApJ 288, 481
Filippenko A.V. and Greenstein J.L. 1984 PASP 96, 530
Fort B., Mellier Y., Picat J.P., Rio Y., Lelièvre G. 1986, Proc. SPIE 627, 321
Kent S.M. 1985 PASP 97, 165
Kowalski M.P., Ulmer M.P., Cruddace R.G. and Wood K.S. 1984, ApJS 56, 403
McMillan S.L.W., Kowalski M.P. and Ulmer M.P. 1989 ApJS 70, 723
Mellier Y. 1989 Proceedings of the Space Telescope Science Institute on "Clusters of Galaxies". Baltimore, USA. May 15-17. M. Fitchett Ed
Mellier *et al.* 1991, in preparation
Oke J.B. 1974, ApJS 27, 21
Owen F.N., White R.A., Hilldrup K.C. and Hanisen R.J. 1982, AJ 87, 1083

Pelló R., Le Borgne J.F., Mathez G., Mellier Y., Sanahuja B., and Soucail G. 1989, Proceedings of the Toulouse Workshop on Gravitational Lensing, Y. Mellier, B. Fort, G. Soucail Eds. (Berlin: Springer) p. 293
Pelló R., Le Borgne J.F., Soucail G., Mellier Y. and Sanahuja B. 1991, ApJ, 366, 405
Rocca-Volmerange B. and Guiderdoni B. 1988 A & AS 75, 93
Sandage A. and Walker M.F. 1966; ApJ 143, 313
Soucail *et al.* 1991, in preparation
Stones R.P.S. 1977, ApJ 218, 767
Thuan T.X. and Gunn J.E. 1976, PASP 88, 543
Ulmer M.P., Kowalski M.P. and Cruddace R.G. 1986, ApJ 303, 162

TABLE 3. *Photometry in the field of Abell 2390.*

id.	x	y	B_j	g	r	B_j-g	g−r	B_j-r	B_b	R_b	B_b-R_b
1	62.7	-191.7	21.87	20.96		0.12					
2	72.5	-188.9	23.94	23.64	23.01			0.48			
3	5.8	-186.8	23.71	22.65	21.46	1.10	0.95	2.03			
4	-21.4	-186.3	23.80	23.13	23.99			1.14			
5	69.8	-185.5	23.30	22.91		0.51					
6	45.6	-185.4	23.45	22.34	21.67	1.29	0.38	1.60			
7	-56.7	-183.7		22.84							
8	19.3	-181.8	22.56	21.69	21.27	0.81	0.24	1.06			
9	-15.5	-181.7	21.69	21.20	20.90	0.51	0.28	0.80			
10	75.6	-180.7	24.00	23.01	23.43	0.82	0.21	0.65			
11	10.4	-180.4	18.09	17.16	17.10	0.93	0.06	0.99			
12	-68.3	-179.7	21.89	20.48	20.05	0.40	0.99	1.42			
13	88.7	-178.4	21.51	20.65	19.54	0.91	1.09	1.95			
14	49.3	-177.2	18.69	17.81	17.58	0.88	0.24	1.12			
15	88.4	-172.4	23.47	22.67	22.13	0.57	0.50	1.19			
16	-80.3	-166.7		20.43	19.28		1.20				
17	98.1	-166.4		23.47	22.20						
18	-70.8	-165.3		22.59							
19	31.3	-162.4	23.09	22.32	21.30	1.34	0.91	1.90			
20	-53.5	-161.6	21.96								
21	-17.4	-158.9	23.91	23.28	22.85	1.26	0.63	1.51			
22	-10.2	-152.3	21.54	20.64	20.06	0.88	0.54	1.44			
23	10.9	-150.1	21.14	20.29	18.93	0.89	1.33	2.22			
24	-6.5	-148.6	23.62	23.15	23.03			0.67			
25	14.8	-148.4	23.54	22.90		0.90					
26	-0.5	-147.4	23.99	23.59	22.91			1.25			
27	7.3	-146.0	21.68	20.86	19.46	0.93	1.29	2.22			
28	-44.8	-145.1	22.05	21.03	19.75	0.98	1.26	2.24			
29	-8.1	-143.6		23.94	22.44						
30	9.1	-140.8		23.37	22.41		1.42				
31	15.0	-138.7	23.57	22.94	21.96	0.69	1.25	1.64			
32	-13.8	-135.8	19.25	18.40	17.71	0.85	0.70	1.55			
33	-64.3	-135.7	23.05	23.07	21.87	0.77	0.96	1.51			
34	48.5	-135.6		22.15	22.59		-0.62				
35	-20.9	-135.3	22.87	22.10	20.72	0.90	0.96	1.93			
36	-5.4	-135.2	22.88	22.14	21.38	0.63	0.75	1.39			
37	83.4	-134.6	21.73	21.16	21.03	0.55	0.14	0.72			
38	78.2	-131.7	22.65	21.67	20.75	0.87	0.95	1.84			
39	18.0	-131.5		23.51	23.45						
40	-10.9	-129.9	21.65	20.71	19.82	0.86	0.96	1.82			
41	93.7	-127.2	22.32	21.81	21.14	0.31	0.37	0.70			
42	14.5	-126.2	21.57	21.22	21.09	0.45	0.02	0.48			
43	179.9	-124.7	22.53								
44	171.3	-123.2	24.39								
45	-111.3	-123.1	23.53								
46	-69.0	-120.3	21.83	20.88	19.67	0.96	1.12	2.07			
47	88.4	-119.5			22.57						
48	-141.2	-119.3	21.95		19.74			2.19			
49	-172.7	-118.8	22.57		20.55			1.75			
50	63.3	-117.4	23.51	22.95	22.13	0.52	0.35	0.88			
51	58.7	-117.3	22.83	21.72	20.69	1.00	1.00	1.99			
52	171.7	-117.2	23.37		22.56			1.13			
53	-89.2	-116.8	24.21		22.50			2.06			
54	-164.0	-116.8	23.65		22.77			0.85			
55	-62.6	-116.4			23.27						
56	134.9	-116.2	24.64		22.77			1.86			
57	-56.7	-116.1	23.12	22.48	22.06	0.26	0.54	0.80			
58	-12.1	-115.9	22.51	22.07	21.66	0.55	0.17	0.87			
59	121.8	-115.5	22.93	22.10	21.55	0.94	0.33	1.26			
60	-76.8	-115.2	22.45	24.47							
61	-82.9	-114.5	24.45	23.46							
62	109.1	-114.3	23.74	23.26			0.29				
63	-80.8	-114.2	24.14		21.55						
64	67.4	-113.6	23.72	23.07	21.81	0.89	0.74	1.70			
65	49.5	-113.6	22.57	21.62	20.16	0.94	1.28	2.30			
66	78.7	-113.3	24.05	22.98	21.75	2.38	0.59				
67	-41.9	-112.7	20.98	20.04	18.75	0.93	1.32	2.14			
68	-122.3	-110.7	22.08		20.44			1.66			
69	33.3	-110.0	24.67								
70	-7.3	-109.8	23.69	23.01	22.84	0.57	0.47	0.86	22.13		
71	78.7	-109.2	20.92	20.21	19.53	0.71	0.63	1.43			
72	182.4	-109.1	22.66		21.74			0.06			
73	-41.5	-106.9	23.42	22.63	21.05	0.85	1.36	2.16	23.58		
74	-85.7	-106.6	26.82		22.99						
75	-107.0	-104.9	23.27		20.99			1.94			
76	-92.3	-104.3			22.62						
77	140.1	-103.6	23.03		21.22			1.70			
78	-64.1	-103.0	24.41	23.77	25.24						
79	2.6	-103.0								23.78	
80	-110.1	-102.3	22.59		20.33			2.16			
81	-129.1	-102.0	22.47		20.27			2.23			
82	167.1	-101.2	24.77		22.14			1.88			
83	-83.5	-99.8	20.16		18.55			1.59			
84	-70.9	-99.7	24.03	24.90							
85	28.9	-97.2	22.60	21.53	20.26	0.98	1.08	2.02	22.93	20.25	2.67
86	-164.3	-96.8			22.46						
87	-77.4	-96.5	24.38	24.07	23.22			-0.35			
88	115.8	-96.2	22.89	21.91	20.88	0.82	1.02	1.85			
89	-5.0	-95.5	23.84	22.74	21.33	1.13	1.36	2.56	23.68	21.26	2.40
90	-42.2	-95.1								23.59	
91	-34.1	-95.0	25.22		23.64					23.52	
92	128.7	-94.4	23.43	22.68	21.64	0.88	0.75	1.61			
93	38.5	-93.3		23.53	21.84				24.46	21.77	2.70
94	-7.1	-92.5								24.52	
95	34.4	-92.5	23.97	22.89	22.25	1.45	0.06	1.52	24.14	22.33	1.60
96	-77.8	-91.3	23.06	23.13							
97	72.0	-90.6	20.25	19.46	18.39	0.82	1.09	1.91			
98	-134.9	-90.0	22.61		20.44			2.12			
99	120.6	-89.7	24.44		23.73			0.81			
100	-53.8	-89.6	24.58		24.87			0.97	25.20	20.04	2.36
101	97.1	-89.2			22.80						
102	170.8	-88.8	24.34		22.80			0.42			
103	-25.1	-88.6								23.43	
104	20.6	-88.5	20.23	19.67	19.44	0.58	0.26	0.87	20.40	19.18	1.24
105	78.2	-87.7	23.59	22.74	21.56	0.57	1.22	1.77			
106	-91.5	-86.9	24.58		24.45						
107	-120.3	-86.4	19.37		18.38			0.98			
108	-28.6	-85.7	22.23	21.25	20.00	0.97	1.19	2.16	22.56	20.03	2.43
109	-66.9	-85.4	23.36	22.68	21.51	0.79	0.87	1.67			
110	-111.9	-85.1	22.76		20.37			2.23			
111	-168.6	-83.9	20.44		18.13			2.25			
112	56.1	-83.8							23.48	23.03	1.54
113	-20.6	-82.6	24.01		23.39					24.28	
114	-99.7	-82.1	23.98		23.14			0.88			
115	-140.4	-81.4	18.57		17.64			0.93			
116	-14.6	-81.4	22.77	21.65	20.40	1.16	1.15	2.28	23.13	20.46	2.61
117	-103.3	-81.2	23.56		22.25			0.92			
118	-162.4	-81.0	21.93		19.60			2.27			
119	86.5	-80.9	23.08	22.24	21.04	0.82	1.00	1.81			
120	-36.3	-80.2	22.28	21.35	20.16	0.95	1.13	2.10	22.59	19.98	2.50

TABLE 3. *(continued)*

id.	x	y	B_j	g	r	B_j-g	g−r	B_j-r	B_b	R_b	B_b-R_b
121	-111.9	-80.2	24.35		23.59			1.26			
122	-46.2	-80.1	23.88	22.92	21.85	0.85	0.92	1.87	24.04	21.74	2.30
123	-71.2	-79.7	21.99	21.38	20.18	0.60	1.16	1.77			
124	20.3	-79.5	23.57	22.94	21.45	0.95	1.07	2.10	23.94	21.57	2.38
125	-51.8	-79.3							25.05	23.86	1.20
126	9.1	-78.9	22.86	21.87	20.67	0.88	1.07	1.98	23.20	20.65	2.44
127	-95.2	-78.4	24.35		21.97			2.10			
128	98.9	-78.0	21.33	20.53	20.02	0.76	0.46	1.23			
129	-132.7	-78.0	21.38		19.31			2.15			
130	-101.9	-77.6	24.02		23.66						
131	-174.4	-77.4	25.17		22.51						
132	-127.3	-76.6			22.08						
133	129.7	-76.4	24.12	23.45	23.03			1.23			
134	-153.6	-76.3	22.23		21.29			0.61			
135	36.9	-76.3	23.74	23.30		0.81			24.11	23.28	1.01
136	-55.3	-76.0			23.16						
137	111.2	-76.0	23.08	22.91	22.57	1.18	0.03	0.69			
138	-52.0	-76.0	23.40	22.32	21.38	1.25	0.81	1.95	23.92	21.09	2.22
139	-93.0	-75.8	22.62		22.10			0.53			
140	-122.8	-75.5	24.29								
141	-104.1	-75.0			23.51						
142	-73.4	-74.8	23.59	23.01		0.55					
143	-28.8	-74.7	24.59		22.78				25.48	22.71	2.44
144	26.2	-74.7	22.69	21.88	21.40	0.81	0.43	1.26	23.24	21.32	1.83
145	-66.7	-74.2	24.93	24.54							
146	7.6	-73.9							25.66	23.59	2.23
147	-112.5	-73.1	22.63		20.48			2.07			
148	-144.8	-73.1	24.97		24.47			2.07			
149	182.3	-72.7	18.60		17.21			1.39			
150	-87.1	-72.5	25.08		23.21						
151	-121.0	-72.2	24.83		22.08			2.32			
152	7.5	-71.9	21.81	20.99	19.76	0.87	1.12	2.00	22.22	19.62	2.60
153	169.1	-70.9	22.34		21.06			1.28			
154	-127.5	-70.8	22.12		19.75			2.20			
155	0.0	-70.4	21.64	20.75	19.43	0.91	1.19	2.08	21.97	19.32	2.58
156	-160.9	-70.2	24.86		24.30						
157	-67.2	-69.6			23.77						
158	-44.7	-68.9	21.65	20.88	19.53	0.78	1.25	2.03	22.45	20.06	2.35
159	-25.7	-68.6		24.13	24.32					24.23	
160	-142.8	-67.4	25.80		23.34						
161	-102.0	-66.4	23.16		21.05			1.69			
162	45.7	-66.2								23.63	
163	-108.1	-65.5	18.56		17.41			1.15			
164	-5.3	-65.3	22.84	22.09	21.55	0.76	0.50	1.32	23.06	21.46	1.69
165	-57.5	-65.2	25.56	23.99					24.94		
166	176.4	-65.0	20.71		18.64			2.09			
167	-126.1	-64.1	21.77		19.34			2.35			
168	-148.5	-63.3	23.05		21.01			2.07			
169	-172.8	-62.5	21.79		19.57			2.23			
170	-19.0	-62.4		22.20	21.29		0.77		24.72	22.51	2.15
171	13.3	-62.4	24.07	23.19	21.62	1.57	1.23		24.21	21.71	2.44
172	-93.7	-62.0	24.06		21.48			2.17			
173	73.9	-61.1	20.88	20.11	19.09	0.79	1.07	1.82			
174	-143.7	-60.3	21.97		19.69			2.18			
175	-110.8	-60.3	22.79		20.39			2.15			
176	-63.3	-59.9	21.24	20.33	19.69	0.89	0.64	1.53	20.23		
177	-58.8	-59.3							24.84		
178	-48.5	-59.1	23.45	22.82	21.35	0.56	1.48	2.32	24.08	21.46	2.56
179	29.0	-59.0	22.37	21.42	20.09	0.99	1.23	2.23	22.60	19.90	2.65
180	7.5	-58.6								23.55	
181	-75.1	-58.2	23.40	22.53	21.74	0.88	0.91	1.76			
182	-100.2	-58.1	21.75		19.65			2.10			
183	148.6	-57.8	22.79		22.84			0.36			
184	44.1	-57.2	23.26	22.61	21.37	0.72	1.05	1.78	23.92	21.35	2.55
185	-135.8	-57.1	22.80		20.40			2.27			
186	-124.3	-57.0	23.73		23.79			0.55			
187	168.6	-56.9	24.69								
188	-15.5	-56.7							23.02	21.69	1.71
189	101.7	-56.4	22.90	22.10	20.72	0.81	1.43	2.16			
190	170.2	-56.1			22.92						
191	37.4	-55.7		23.99	23.70				24.84	22.94	1.89
192	-54.4	-55.6	21.48	20.60	19.42	0.86	1.22	2.09	21.97	19.19	2.41
193	1.1	-55.3	23.89	22.88	21.93	0.40	1.38	1.74	24.09	21.83	2.15
194	32.3	-54.9								23.72	
195	11.9	-54.9	24.01	23.02	21.83	1.09	-0.07	1.00	24.13	21.74	2.41
196	-160.1	-54.4	21.11		20.34			0.52			
197	-62.6	-54.4	23.75	23.09	22.31	0.90	1.06	1.50	21.39		
198	-39.7	-53.5			22.08				25.03	22.73	2.46
199	41.7	-53.4	23.73	22.93	22.44	0.38	0.69	1.02	24.34	22.57	1.53
200	-120.4	-52.7	23.18		22.15			0.33			
201	-23.9	-52.4	16.63	15.64	16.13	0.99	-0.37	0.63			
202	51.1	-52.3		23.04	21.86				24.97	22.29	2.63
203	-138.7	-51.4	21.31		19.08			2.17			
204	59.5	-51.4	24.20		22.30			1.71			
205	144.6	-51.3	23.50		22.68						
206	12.0	-51.3							24.85	22.96	2.70
207	57.4	-51.1	23.70	23.26	22.35			0.86		22.19	
208	-79.5	-50.8	24.23	23.14	21.94	1.47	1.23	2.48			
209	51.2	-50.5	22.84	22.41	21.64	0.60	0.09	0.98	23.18	21.79	1.39
210	18.6	-50.2	23.53	22.74	21.32	0.86	0.92	2.05	23.89	21.32	2.55
211	68.9	-50.2	23.49	22.40	21.42	1.21	0.75	1.91			
212	-144.2	-49.1	20.81		18.96			1.82			
213	125.6	-48.2	16.68	15.64	15.76	0.95	-0.13	0.92			
214	-71.2	-47.9			24.08						
215	-120.3	-47.9	21.78		19.56			2.20			
216	152.8	-47.5	21.94		19.74			2.28			
217	-130.0	-47.0	24.47		23.46						
218	-48.5	-46.4	22.89	22.57	22.56	0.43	-0.16	0.38	23.71	23.46	0.64
219	-153.4	-45.2	21.73		19.58			2.22			
220	-93.1	-44.8	19.05		18.07			0.98			
221	-43.4	-43.8	23.62	25.67	25.48			0.08	24.70	23.55	1.57
222	28.3	-42.3	21.83	21.02	20.75	0.76	0.29	1.05	22.46	20.89	1.52
223	-53.5	-42.3	22.35	21.48	20.19	0.87	1.28	2.18	22.80	20.07	2.67
224	-106.4	-41.8	24.61		22.35						
225	-134.6	-41.5	22.59		20.36			2.53			
226	-86.1	-40.5	25.44		22.71						
227	37.9	-39.6	22.69	21.73	20.58	0.95	1.04	2.03	22.93	20.49	2.44
228	-20.5	-38.8	22.10	23.84					24.87	24.08	1.10
229	-125.7	-38.7	21.89		19.78			2.07			
230	-52.4	-38.6								23.65	
231	158.4	-38.5	23.31		23.80						
232	-140.4	-38.4	22.51		21.87			0.60			
233	-107.7	-37.7	23.54		23.09						
234	-135.7	-37.2	23.72		22.46			1.23			
235	-80.3	-37.0	24.99		23.78						
236	-34.0	-37.0	22.33	21.31	20.02	0.98	1.31	2.31	22.60	19.95	2.62
237	18.3	-36.9								24.41	
238	-89.4	-35.8	23.42		21.75			1.97			
239	-12.0	-35.7	22.32	21.57	20.28	0.80	1.23	2.16	22.82	20.20	2.56
240	20.6	-34.7	21.46	20.56	19.25	0.91	1.28	2.17	22.62	20.11	2.45

TABLE 3. *(continued)*

id.	x	y	B_j	g	r	B_j-g	g−r	B_j-r	B_b	R_b	B_b-R_b
241	-16.8	-34.3	24.68	23.95	23.25				24.77	23.20	2.56
242	99.2	-34.3	23.22	22.47	22.21	0.73	0.16	0.88			
243	13.9	-33.5							24.22	22.85	2.28
244	24.0	-33.4							25.35	23.73	1.67
245	-150.3	-33.1	23.45		22.01			1.01			
246	138.3	-32.5	22.59		22.07			1.03			
247	-7.6	-32.3	22.40	23.73					23.32		
248	9.0	-31.7	20.77	19.87	18.56	0.88	1.27	2.18	21.34	18.61	2.60
249	182.1	-31.7	23.68		21.47			1.94			
250	89.9	-30.9	23.00	22.23	21.07	0.64	1.35	2.02			
251	85.9	-30.7	24.58	23.70	22.34						
252	-137.5	-30.7	25.64		22.36						
253	-96.9	-30.6	23.80		21.87			1.61			
254	22.4	-30.4								23.87	
255	-40.0	-29.0	20.43	19.87	19.56	0.74	0.09	0.87	20.85	19.37	1.48
256	42.0	-28.6	23.14	22.80	21.64	-0.27	1.53	1.27	23.10	21.50	2.03
257	130.5	-28.4	25.76	25.50							
258	127.7	-28.3			24.85						
259	83.4	-27.6		23.42	22.63		0.85				
260	-90.2	-27.2	22.38		20.20			1.97			
261	8.5	-27.2	22.82	22.19		0.90			23.86	21.20	2.27
262	170.1	-27.1	22.94		22.01			0.96			
263	44.1	-26.9		22.97					23.82	23.07	1.87
264	120.7	-26.6	23.21	22.35	21.18	0.98	1.24	2.21			
265	-163.2	-26.5	21.47		19.11			2.31			
266	-100.7	-26.4	25.24		24.40						
267	-9.4	-26.1							25.52	24.45	2.31
268	3.3	-24.1								24.84	
269	31.6	-23.8			22.98					23.22	
270	78.7	-23.3	19.99	19.31	18.91	0.64	0.45	1.09			
271	-2.0	-22.9								24.09	
272	-67.0	-22.5	22.38	23.80							
273	58.2	-22.5	22.17	21.42	19.96	0.78	1.40	2.14		19.29	
274	-125.9	-22.3	23.84		21.73			2.28			
275	-10.3	-22.0	21.33	20.40	18.86	0.93	1.41	2.45	21.56	18.69	2.82
276	32.9	-22.0	23.53	23.37		0.40					
277	-78.9	-21.7	21.84	20.82	19.44	1.06	1.20	2.28			
278	-14.2	-21.6							24.06	21.50	2.50
279	145.4	-21.3	22.63		20.90			1.76			
280	-76.7	-21.0	22.01	21.29		0.97					
281	-37.8	-20.8	24.48	23.45	22.14			1.94	24.64	22.11	2.30
282	-151.7	-20.7	25.01		21.59						
283	4.5	-20.6	23.63	22.62	21.41	1.13	0.88	2.06	23.87	21.24	2.61
284	80.6	-19.8	21.63	20.77	19.58	0.88	1.15	2.09			
285	27.3	-19.7								24.02	
286	-12.4	-19.6	21.95	20.95	18.84	0.98	1.41	2.39	22.46	19.61	2.80
287	-156.1	-19.5	22.33		20.34			2.02			
288	30.7	-18.6		23.90	24.06				25.45	24.46	1.32
289	20.6	-18.3		24.42	25.02				25.25	23.58	1.65
290	122.4	-18.2	17.72	16.88	16.83	0.84	0.05	0.85			
291	69.0	-18.0	24.14		24.20			0.62			
292	86.1	-17.5	22.37	23.82							
293	136.4	-17.3			25.25						
294	-98.8	-17.0	23.46		21.65			1.71			
295	82.7	-16.9	22.75	21.70		0.91					
296	65.5	-16.8		23.31	25.45		-0.27				
297	45.7	-16.2	21.56	20.54	19.17	0.99	1.37	2.33	21.77	18.95	2.73
298	-126.6	-15.5	20.83		18.60			2.22			
299	-64.1	-15.3	22.11	21.52	20.35	0.65	1.17	1.72	21.50		
300	-79.2	-14.9	24.58	24.67	23.30			0.47			

id.	x	y	B_j	g	r	B_j-g	g−r	B_j-r	B_b	R_b	B_b-R_b
301	-4.2	-14.3	25.47	25.87	22.71					23.58	
302	-50.0	-13.7		23.80	21.44						
303	-75.2	-13.6			25.26						
304	168.3	-13.1	23.76		23.12			1.45			
305	55.1	-12.9								24.13	
306	-51.5	-12.1	23.34	22.53	21.37	0.47	1.34	1.80	23.75	21.39	2.21
307	50.8	-12.1			23.04				25.17	23.71	1.11
308	107.3	-11.6		23.92	24.21						
309	23.3	-10.8								23.55	
310	115.7	-10.4	21.39	20.61	19.36	0.80	1.17	2.00			
311	-147.3	-9.7	23.97		21.84			1.80			
312	25.4	-9.1		25.37	23.50					23.90	
313	-84.2	-9.1	19.82		17.99			1.76			
314	-13.6	-8.8	23.08	21.40	20.82	1.65	0.51	2.05	23.58	20.93	2.62
315	77.5	-8.5	20.92	20.08	19.08	0.80	1.02	1.82			
316	-153.9	-8.0	24.52		21.16			2.79			
317	-141.8	-7.7	22.79		20.95			1.86			
318	46.0	-6.8		23.95	23.17					22.86	
319	-114.2	-6.4	23.75		21.59			2.05			
320	-96.6	-6.3	21.67		19.40			2.20			
321	122.5	-6.3		24.62	22.29						
322	24.0	-6.2		25.83	23.09					23.26	
323	-82.4	-5.2	21.79		19.67			2.22			
324	28.3	-4.8	25.27	22.45	21.08	1.17	1.09	2.14	24.26	21.25	2.58
325	21.0	-4.0	23.09	25.71	25.68					23.64	
326	-88.5	-3.9	23.49		21.08			2.18			
327	161.3	-3.4	23.49		22.81			1.06			
328	1.6	-3.0							22.86	20.42	2.44
329	29.5	-2.6							25.48	22.57	2.50
330	-1.0	-2.5								19.55	
331	85.4	-2.5		23.70	22.51						
332	-19.0	-2.5	23.19	24.72							
333	-160.7	-2.1	24.64		21.75			2.08			
334	66.0	-2.0	18.64	17.80	17.51	0.83	0.30	1.13			
335	-103.0	-1.9	22.88		21.81			1.09			
336	36.0	-1.7		24.14					25.61		
337	-9.6	-1.5	21.19	20.27	18.92	0.90	1.28	2.21	21.76	19.28	2.37
338	-22.8	-1.5	22.88	21.78	19.99	1.43	1.60	2.89	24.19	20.59	2.99
339	42.0	-0.9	23.33	22.44	21.09	0.95	1.02	1.99	23.58	21.03	2.50
340	-25.1	0.0							24.50	21.77	2.24
341	0.0	0.0	19.58	18.59	17.55	0.95	1.05	2.02	20.47	17.99	2.46
342	-32.6	0.1	23.60	24.96	24.72			0.74	25.37		
343	7.7	0.5		22.28	20.50		1.23		25.10	21.43	2.92
344	35.5	0.5	23.75	22.97	21.51	1.72	0.81	2.36	24.20	21.43	2.72
345	17.9	0.9	23.11	22.04	20.82	0.96	1.01	2.07	23.55	20.92	2.58
346	-123.9	1.0	20.28		18.49			1.78			
347	-91.5	2.3	22.82		20.59			2.16			
348	169.7	2.3	21.31		18.96			2.31			
349	49.1	2.4	24.71	23.15	22.50				25.35	22.50	2.26
350	-23.5	2.6	21.41	20.41	19.05	0.96	1.23	2.19	21.93	19.31	2.54
351	-57.2	3.1	24.23	23.20	22.09	1.42	0.42	1.68	24.17		
352	-84.7	3.2	23.92		22.17			1.61			
353	-87.0	3.5	23.14								
354	-61.5	4.2		23.93	23.11						
355	32.5	4.5	23.27	22.23	20.87	0.87	1.12	1.98	23.39	20.88	2.41
356	16.7	5.3	22.65	21.36	20.31	1.02	1.17	2.18	23.44	20.87	2.49
357	180.0	5.6	23.68		22.56			0.80			
358	14.3	5.6	23.54						25.74	23.04	2.68
359	39.5	5.7		24.41	23.37				25.41	22.95	2.15
360	52.3	5.9	22.64	21.66	20.47	0.88	1.18	2.09	23.05	20.42	2.54

TABLE 3. *(continued)*

id.	x	y	B_j	g	r	B_j-g	g−r	B_j-r	B_b	R_b	B_b-R_b
361	-174.7	6.1	23.44								
362	-67.4	7.1	22.83	21.93	21.73	0.93	0.25	1.18			
363	-84.0	7.3	21.51		19.23			2.18			
364	23.1	7.5	21.60	20.60	19.13	1.03	1.38	2.37	21.87	19.15	2.64
365	-15.5	7.7	22.38	21.55	20.13	1.12	1.14	2.27	22.99	20.15	2.77
366	-88.0	7.9	23.95								
367	48.2	9.0		25.40						23.30	
368	-45.6	9.0	17.81	17.00	17.02	0.81	-0.03	0.79	17.33	15.91	1.42
369	9.8	9.4	24.52						23.70	22.96	1.41
370	-27.6	9.4							24.31	22.50	1.82
371	-26.3	9.4	22.08	21.50	20.21	0.61	1.23	1.84	22.83	20.15	2.63
372	-63.4	10.1		24.10	23.48				21.58		
373	-31.6	10.1	24.68	23.87	23.46				24.72	23.73	1.02
374	1.1	10.5	22.61	21.82	20.36	0.87	1.28	2.15	23.39	20.65	2.68
375	-96.7	11.0	23.39		21.19			1.99			
376	107.6	11.5		23.91	21.59						
377	-141.6	11.6	23.48		22.88			0.87			
378	21.8	11.6	22.67	21.57	20.31	1.05	1.17	2.23	22.58	21.75	2.33
379	-171.7	12.3	22.99		22.09			1.00			
380	42.1	12.7	21.93	21.46	21.30	0.77	-0.19	0.62	22.24	21.17	1.04
381	8.0	13.0	23.76	22.81	22.11	0.84	0.63	1.44	24.05	22.01	2.03
382	115.4	13.0	23.24	22.09	20.94	0.88	1.13	2.05			
383	139.4	13.2	20.70		19.85			0.82			
384	-40.3	13.2	22.54						23.45	22.83	0.78
385	130.6	13.6	21.13	20.38	19.83	0.73	0.55	1.26			
386	53.4	14.0	22.80	22.32	21.10	0.47	0.81	1.47	23.37	21.44	1.93
387	0.6	14.1							25.94	23.04	2.78
388	31.6	14.1	20.93	19.96	18.66	0.89	1.34	2.26	21.32	18.64	2.56
389	-71.4	15.1	19.40	18.73	18.44	0.66	0.31	0.92			
390	47.6	15.1	21.14	20.15	18.83	0.94	1.28	2.24	21.41	18.86	2.49
391	16.9	15.5	22.26	21.58	21.06	0.67	0.41	1.04	22.57	21.05	1.46
392	105.6	15.8		24.67	23.62						
393	-154.3	16.1	22.16		20.79			1.30			
394	69.5	16.8	22.08	21.23	20.03	0.83	1.18	1.99			
395	2.7	17.4								24.43	
396	55.1	18.5	23.44	22.52					24.60	23.85	0.77
397	-135.9	18.6	25.24		24.27						
398	-1.7	18.6	25.31								
399	53.6	18.9							25.52		
400	-4.2	19.0		24.47	22.43				24.96	23.72	1.38
401	-45.7	19.2								23.73	
402	37.8	19.7								23.40	
403	32.1	19.7	23.28	22.29		1.44			24.25		
404	4.1	19.8	25.12	23.58	22.14				25.12	22.31	2.70
405	-87.3	20.2	22.08		19.93			2.09			
406	-46.9	20.3	24.86	23.70	22.80			1.27	24.74	23.01	1.75
407	-11.1	20.4							25.04	23.42	1.59
408	57.3	20.5	23.15	21.48	20.26	1.35	1.14	2.29		20.64	
409	26.3	20.6	22.67	22.16	21.19	0.38	0.80	1.18	23.24	21.65	1.65
410	-101.2	20.7	21.64		19.36			2.36			
411	-22.2	21.3	22.88	21.78	20.68	0.96	1.16	1.94	23.10	20.62	2.45
412	5.0	21.6							26.58	23.76	2.26
413	-14.0	22.8	21.89	21.24	20.31	0.77	0.83	1.61	22.11	20.13	1.98
414	19.6	23.0							24.46	23.39	1.07
415	21.3	23.2	22.44	21.73	20.68	0.79	0.98	1.70	23.92	21.31	2.30
416	-32.7	23.7	23.59	22.95	22.48	1.30	0.04	1.25	23.81	22.71	1.18
417	160.0	24.5	22.73		20.51			2.16			
418	58.3	24.8	23.61	23.45							
419	101.3	24.8		23.96	23.87						
420	18.4	25.1							25.62		

id.	x	y	B_j	g	r	B_j-g	g−r	B_j-r	B_b	R_b	B_b-R_b
421	-59.0	26.0	22.06	21.05	19.85	0.97	1.19	2.10	22.78		
422	-26.9	26.1		25.49					25.32	24.72	1.04
423	-174.8	26.2	23.66		23.72			-0.06			
424	50.2	26.8	24.31		23.97						
425	67.1	27.6	23.13	22.16	20.89	0.82	1.16	1.97			
426	28.5	27.9								23.10	
427	112.0	28.7	24.18	23.54	23.08			1.06			
428	-55.0	28.8							26.07		
429	10.8	29.2	22.02	21.18	19.78	0.93	1.38	2.31	22.39	19.66	2.66
430	35.7	29.4	21.58	20.73	19.70	0.83	1.03	1.88	21.82	19.60	2.22
431	-61.5	29.4	23.83	22.66	21.25	0.87	1.26	2.02	21.09		
432	-72.3	30.1	21.64	20.74	19.45	0.93	1.25	2.18			
433	1.8	30.3	23.73		22.72			0.64		21.58	
434	156.4	30.5	22.40		22.14			0.79			
435	31.5	30.8	21.89	20.89	19.48	1.08	1.30	2.29	22.56	19.86	2.66
436	-162.5	30.9	23.99		23.34			-0.07			
437	-0.4	31.0	23.38	23.18	22.56	0.08	0.88	0.88	24.14	22.89	1.47
438	-132.1	31.1	22.47		20.30			2.10			
439	-1.5	31.1	23.38	23.18	22.56	0.08	0.88	0.88	25.60	22.92	2.62
440	122.3	31.2	22.35	21.45	20.14	0.92	1.22	2.14			
441	107.6	31.5	24.61		22.66			0.92			
442	101.9	32.2	24.33	24.54	22.30			1.39			
443	112.6	32.2	23.79	23.24	21.81	0.82	0.80	1.73			
444	72.8	32.3			25.17						
445	47.0	32.3		26.24	25.02						
446	79.2	32.6	24.15	23.19	24.38			0.53			
447	-33.9	32.6	25.80	24.30	22.67				25.07	22.41	2.59
448	-93.6	33.3	25.45		24.80						
449	-25.1	33.8	24.71	24.97	22.83					22.59	
450	-158.9	34.0	23.82		21.54			2.54			
451	138.5	34.2			22.98						
452	57.0	34.8		23.42	22.66					22.80	
453	144.4	35.4	23.60		22.52			1.30			
454	24.0	36.0		25.34	23.26				25.42	22.75	2.32
455	34.4	36.1							25.71	23.20	2.38
456	7.7	36.3	25.60		23.29				25.04	22.66	1.91
457	99.0	36.6			25.28						
458	182.4	36.9			18.63						
459	83.9	37.5	24.44	22.58	21.82	1.69	0.39	2.04			
460	-48.6	37.5		25.43	25.24						
461	33.6	38.2	23.84	22.70	21.81	0.41	1.06	1.69	23.82	21.80	1.86
463	-8.3	39.2	23.62	23.52	23.37			0.75	23.64	23.99	0.62
464	148.2	39.3	21.24		20.57			0.79			
465	81.7	39.3	24.13	22.94	21.95	2.17	1.29	2.62			
466	30.4	39.4	22.71	22.59	20.29	0.09	2.18	2.21			
467	72.1	39.7		22.85	22.27		0.78				
468	49.2	40.1							24.81		
469	-16.4	40.3	23.70	23.19	22.94	0.39	0.06	0.70	23.96	22.55	1.43
470	26.7	40.8	22.69	21.87	20.34	0.95	1.28	2.35	23.05	20.29	2.65
471	-43.1	41.5	22.41	21.56	20.72	0.85	0.77	1.65	23.19	21.13	2.06
472	-152.9	41.7	22.67		20.46			2.03			
473	-30.0	41.7			24.09					23.69	
474	17.8	41.8	23.69	23.08	24.43	1.01		0.03	23.85	23.18	0.83
475	-60.0	41.9	23.45	22.49	21.22	0.87	1.09	1.97	23.82		
476	-77.4	41.9	22.90	22.22	21.30	1.24	0.59	1.50			
477	47.7	42.1	21.74	21.19	20.84	0.61	0.31	0.92	22.54	21.36	1.18
478	157.9	42.1	17.58		16.70			0.89			
479	166.1	42.2	22.58		21.54			1.25			
480	75.4	42.5	22.79								
481	-33.8	42.7	24.71	25.65	23.59		-	-0.65		22.93	

TABLE 3. *(continued)*

id.	x	y	B_j	g	r	B_j-g	g−r	B_j-r	B_b	R_b	B_b-R_b
482	-9.0	42.9			23.92				26.67	23.37	2.96
483	3.0	42.9		23.92	22.88				25.79	22.73	3.00
484	99.3	42.9			23.45						
485	-76.6	43.0	23.28	22.44	21.09	0.68	1.37	2.23			
486	43.2	43.0	21.58	20.77	19.89	0.79	0.82	1.62	22.63	20.04	2.41
487	7.2	43.3		25.28	23.41						
488	-12.3	43.6	25.51	24.52					25.16	23.72	1.43
489	-25.4	43.7			24.31						
490	-69.9	44.9	23.53	22.36	21.41	0.96	0.98	1.95			
491	51.4	45.6			22.83					22.80	
492	-56.1	45.7	23.15	22.31	21.03	0.97	1.11	2.08	23.32	19.81	2.41
493	119.1	46.0			23.39						
494	-165.2	46.3	21.48		20.50			1.00			
495	75.6	46.6	21.11	20.18	18.77	0.94	1.33	2.29			
496	31.6	46.6	24.78	23.30	22.19	2.16	0.61		24.32	22.06	2.13
497	-41.9	46.8	22.98	22.01	21.16	0.92	0.79	1.71	23.35	20.89	2.43
498	42.4	46.8	22.76	21.76	20.51	0.98	1.25	2.32	23.17	20.51	2.59
499	16.5	46.9	24.29	23.39	22.25			2.04	24.54	22.06	2.43
500	24.9	46.9								23.93	
501	-115.1	46.9	24.09		22.77			2.35			
502	-13.9	47.0								22.59	
503	-15.0	47.6	22.92	22.34	21.60	0.47	0.48	0.93	23.11	21.74	1.40
504	-107.7	47.9	22.92		21.68			1.02			
505	3.1	48.8	24.35	23.23	25.59			-0.26	24.34		
506	7.2	49.2							25.13	24.41	0.84
507	-30.0	49.2								23.48	
508	138.7	49.8	22.13		21.47			1.19			
509	-57.7	50.0			24.96				24.50		
510	7.4	50.2	25.47	24.01	23.24				25.03	23.72	1.47
511	-138.5	50.5	23.81		21.72			1.81			
512	-80.8	50.8	24.67	24.52							
513	100.0	50.8	21.59	20.71	19.35	0.87	1.24	2.12			
514	54.7	51.3	24.17	23.30	22.02	1.27	0.87	2.13	23.89	21.78	2.36
515	-78.2	51.5	25.51	25.49	23.49						
516	-145.7	52.1	22.45		20.16			2.33			
517	170.4	52.3	23.60		21.59			1.65			
518	21.3	52.3							25.68		
519	72.8	52.4	21.02	20.18	19.13	0.98	0.91	1.89			
520	-68.1	52.9	22.99	22.26	21.12	0.47	1.24	1.64			
521	3.4	53.5	24.28	25.66					25.42		
522	15.1	53.5	22.43	21.94	21.33	0.38	0.61	1.11	22.72	21.23	1.49
523	25.2	53.8	23.09	22.58	21.73		2.17	1.19	23.41	21.49	1.91
524	-174.2	53.8	19.57		18.86			0.65			
525	116.2	54.0	19.30								
526	-10.8	54.5	24.85	25.93	24.73						
527	113.6	54.6	19.35	18.73	18.39	0.61	0.35	0.99			
528	33.0	55.0							25.47	24.24	1.23
529	64.2	55.2	24.49	23.84	23.23			0.42			
530	106.8	55.2	21.62	20.70	19.29	0.91	1.41	2.32			
531	44.3	56.0		23.83	23.52				25.36	23.04	1.94
532	139.1	56.1	23.37		21.78			1.65			
533	177.0	57.2	22.03		19.79			2.17			
534	-158.6	57.8	21.05		18.85			2.14			
535	92.8	58.3	23.75	22.54	21.42	1.02	0.85	1.87			
536	128.6	58.8	22.65	22.05	21.26	0.45	0.81	1.37			
537	-96.5	59.6	23.86		23.35			0.59			
538	112.0	59.7	23.03	22.37	21.50	0.57	0.55	1.22			
539	-3.7	60.5	23.91	23.26	23.37	1.04	-0.34	0.63	24.55		
540	-7.7	61.4	26.18		23.37					23.12	
541	109.0	62.2			21.35						

id.	x	y	B_j	g	r	B_j-g	g−r	B_j-r	B_b	R_b	B_b-R_b
542	31.1	62.4								23.83	
543	50.0	62.5	23.08	22.13	21.02	0.81	1.02	1.82	23.49	20.95	2.43
544	130.1	62.6	23.17	22.59		0.69					
545	94.3	62.6		24.23	23.33						
546	-65.9	62.7	24.02		23.27						
547	-27.5	63.6							24.34	22.65	2.24
548	-12.7	64.1	24.22	23.81	22.45				0.01	23.71	22.86	1.49
549	-68.7	64.7	25.01	22.56	23.20	1.86	0.20	2.42			
550	54.7	64.9	22.74	21.59	20.58	1.48	0.58	2.04		20.89	
551	-83.5	65.1	22.35	21.76	21.17	0.60	0.49	1.11			
552	-174.6	65.1	21.29		19.48			1.76			
553	25.0	65.5	22.21	21.27	19.82	0.87	1.44	2.24	24.34	22.03	2.24
554	-72.3	65.6	24.65	25.35							
555	16.1	65.8			23.28						
556	22.8	66.2	22.15	21.29	19.90	0.84	1.40	2.19	22.51	19.83	2.64
557	60.7	66.4	22.56	21.78	20.57	0.77	1.17	1.95		19.89	
558	108.2	66.8	18.60	17.91	17.89	0.68	0.05	0.68			
559	-135.4	67.3	18.83		17.94			0.89			
560	54.4	67.4	21.23	20.35	19.29	0.85	1.15	1.88	21.27	19.25	2.13
561	85.3	67.8	23.93	23.05	21.66	0.92	1.13	1.83			
562	49.8	67.8			23.81						
563	96.2	69.0	22.77	21.75	20.70	1.01	1.02	2.04			
564	-48.8	69.2								23.87	
565	-153.8	69.5	23.44		22.66			0.83			
566	-57.4	69.8	23.95	23.22	23.36	0.03	0.23	0.34			
567	2.4	70.2								24.09	
568	-83.9	70.4	22.58		20.35			2.09			
569	40.8	70.8	22.72	21.69	20.48	1.04	1.13	2.10	23.10	20.45	2.55
570	114.3	71.2	21.03	19.76	18.36	1.19	1.41	2.27			
571	16.5	71.9		22.17	24.20					24.19	
572	-113.0	72.0	24.28		22.03			2.02			
573	4.0	73.0		24.07	23.29						
574	111.1	73.9	21.25	20.90		0.31					
575	-30.4	73.9	25.75	24.68	25.20				24.69	24.11	0.88
576	158.7	73.9	22.78		20.97			1.84			
577	77.4	74.2	23.82	23.65	23.88	0.30	-0.45	0.31			
578	-60.9	74.3	23.79	22.57	22.28	1.22	0.62	2.35	24.40		
579	126.7	75.3	19.99	19.23	18.47	0.73	0.78	1.50			
580	98.6	75.4	22.08	21.11	20.28	1.03	0.68	1.72			
581	-136.2	75.7	23.26		23.03			0.38			
582	-162.2	75.8	23.48		20.73			2.47			
583	-70.0	75.9	18.39	17.56	17.41	0.82	0.16	0.99			
584	0.1	75.9							25.36		
585	173.5	76.5	22.12		20.71			1.33			
586	6.5	76.9	25.64		23.41				25.09	22.87	2.21
587	-56.2	77.4	26.13	26.35	23.80						
588	-77.1	77.4	20.95	19.95	18.65	0.94	1.29	2.24			
589	-49.4	78.0	20.86	19.92	18.55	1.14	1.20	2.36	21.28	18.55	2.72
590	25.1	78.3							25.24	25.12	0.49
591	-84.8	78.3	23.14		20.82			1.98			
592	96.7	79.0	22.74	21.91	20.40	0.75	1.43	2.19			
593	183.3	79.1	23.16		22.20			1.12			
594	123.4	81.0	23.24	23.46	20.60			2.30			
595	120.4	81.1	23.38	22.11	20.69	1.10	1.11	2.22			
596	-40.4	81.1		24.42	24.21						
597	-145.0	81.3	23.06		22.95			0.35			
598	36.0	82.3	22.46	22.03	22.07	0.56	-0.03	0.47	22.86	21.75	1.13
599	-97.2	82.9	22.51		22.18			0.46			
600	-0.4	83.4	22.98	22.94	22.14	0.42	0.46	0.85	23.97	21.85	1.63
601	-6.3	83.5	21.33	20.46	19.22	0.87	1.25	2.13	21.70	19.14	2.54

TABLE 3. *(continued)*

id.	x	y	B_j	g	r	B_j-g	g−r	B_j-r	B_b	R_b	B_b-R_b
602	65.7	84.2	19.69	18.94	18.24	0.75	0.73	1.46			
603	71.1	87.2		24.73	22.22						
604	20.0	88.0	23.60	23.40	23.48			0.26			
605	-29.9	88.3	19.73	18.98	18.34	0.76	0.65	1.39	19.85	17.94	2.16
606	183.7	89.4	22.95		21.86			1.26			
607	-46.0	89.4	25.26	23.44	22.85					21.10	
608	-51.2	89.6	25.61		25.48						
609	104.9	90.2		23.67	22.34						
610	-88.2	90.9			23.43						
611	-13.4	91.0	25.07	23.12	21.81						
612	153.5	91.3	22.13		19.89			2.22			
613	-110.9	92.0	25.91		23.65						
614	77.3	92.2		25.09	23.01						
615	138.2	93.1	24.04		21.71			2.52			
616	129.2	93.4	20.44	19.81	19.57	0.63	0.23	0.87			
617	59.5	94.0	21.98	21.44	21.32	0.59	0.05	0.66		19.63	
618	171.9	94.1	23.00		20.97			1.80			
619	56.8	96.9	23.11	22.13	21.06	0.81	1.15	2.02			
620	79.1	99.0	23.29	22.51	21.82	0.54	0.82	1.37			
621	-12.6	100.2	23.29	22.24	20.70	0.91	1.46	2.38			
622	30.9	100.4	23.06	22.54	21.69	0.50	0.72	1.18			
623	-73.7	100.5	23.62	22.85	21.75	0.66	0.97	1.62			
624	39.3	100.7	21.52	20.79	20.26	0.74	0.56	1.30			
625	-65.8	102.1	22.38	21.82	20.84	0.56	0.98	1.54			
626	124.0	103.0		23.98	22.28						
627	-61.3	103.3	25.82	23.47	22.07						
628	20.8	104.1	24.01	23.08	22.57	0.46	0.96	1.42			
629	-3.6	105.0	23.61	23.54	23.36	0.08	0.00	0.42			
630	76.5	105.6		23.84	25.46						
631	86.5	106.1		25.05	24.52						
632	102.6	107.0		24.63	23.53						
633	-37.2	107.9	22.40	21.59	21.00	0.74	0.48	1.32			
634	-84.4	109.1	24.34		21.91			1.86			
635	-25.9	109.1	24.60	22.30	22.25	2.21	0.04	2.06			
636	65.1	111.4	23.58	22.93	23.56	0.34	0.16	0.29			
637	60.6	111.9	24.32	22.99	21.74	1.24	0.49	1.73			
638	51.6	112.3	23.99	23.80	21.91			1.66			
639	-43.8	116.3	25.79	23.86	25.46						
640	-30.7	116.5	24.45	24.20	25.47			0.13			
641	-0.3	116.9	22.51	22.01	21.02	0.88	0.85	1.69			
642	55.7	117.3		24.99	25.48						
643	75.5	117.9	17.34	16.50	16.59	0.84	-0.08	0.77			
644	109.9	118.4	23.74		23.75			0.29			
645	124.8	119.2	23.21	22.53	21.52	0.58	0.26	0.77			
646	44.6	119.4		23.82	22.11						
647	19.5	119.6		23.98	24.03						
648	121.3	120.1	22.90	22.02	20.68	0.91	1.14	2.05			
649	-51.0	120.2	23.42	22.30	21.43	0.94	0.84	1.77			
650	130.6	120.6	21.11	20.22	18.88	0.84	1.34	2.02			
651	-8.0	121.7	18.75	17.94	17.74	0.81	0.21	1.00			
652	91.2	121.8	24.16	23.40	24.60	1.29	0.80	2.27			
653	1.2	122.0	24.51	23.58	22.31			1.51			
654	85.6	122.5	24.43	24.70	22.88			1.29			
655	6.9	122.6		24.26	22.29						
656	44.7	123.3		23.78	23.90						
657	-19.5	123.9	22.35	21.75	20.56	0.64	1.14	1.82			
658	-39.6	126.6	23.59	23.79	22.05			1.67			
659	105.7	127.0		23.59	22.71						
660	-21.9	127.4	22.54	21.77	21.04	1.25	0.79	1.56			
661	-49.6	127.8	23.65	22.71	21.43	0.83	1.17	2.03			
662	78.7	129.6	23.08	22.25	20.50	0.89	1.64	2.56			
663	-26.1	133.0	22.36	21.65	21.38	0.72	0.27	0.97			
664	25.1	136.4		25.68	23.15						
665	91.6	136.5	21.59	20.59	19.24	1.00	1.35	2.37			
666	132.9	137.0		23.18	21.26		2.24				
667	-36.7	138.3	20.66	19.86	19.00	0.98	0.69	1.69			
668	-63.4	139.9	20.59	19.74	18.50	0.88	1.23	2.12			
669	96.1	140.3	22.37	21.55	21.10	0.73	0.47	1.20			
670	19.6	140.8	23.71	22.61	21.66	1.19	0.73	1.92			
671	-47.3	142.4	22.44	22.06	21.85	0.57	-0.19	0.69			
672	-30.1	144.0	25.57	25.34							
673	127.8	144.7		23.88	22.30						
674	110.5	145.4	23.93	22.87	21.35	1.16	1.70	2.45			
675	-14.9	146.8	21.97	21.12	20.01	0.83	1.13	2.00			
676	50.6	147.3	23.77	23.33	23.03	0.05	0.08	0.81			
677	6.2	147.4	24.35	24.11							
678	-76.1	148.9	23.46	22.74	21.49	1.27	1.26	1.87			
679	0.8	150.1	21.36	20.33	19.04	0.95	1.32	2.29			
680	73.6	150.6		22.88	22.06		1.02				
681	43.5	150.6		24.40	22.51						
682	11.9	150.9		24.29	23.16						
683	-61.0	151.3	21.66	20.89	19.69	0.80	1.11	1.91			
684	-33.2	151.4	23.56	22.71	21.81	0.29	1.47	1.76			
685	79.1	151.6		23.28	23.12		0.08				
686	126.8	154.4	22.16	21.36	20.63	0.51	1.07	1.67			
687	6.7	160.2	21.96	21.18	20.11	0.92	0.88	1.82			
688	41.5	161.1		23.13	21.95		1.33				
689	-29.5	162.1	23.21	22.01	20.87	1.12	1.03	2.14			
690	-16.1	162.1		24.70	23.35						
691	5.2	162.3	22.34	21.30	20.37	1.15	1.00	2.23			
692	123.7	163.4	20.82	19.88	18.77	0.92	1.12	2.04			
693	-72.3	166.2	26.32	25.45	23.98						
694	-2.7	168.0	24.08	23.79							
695	110.2	168.1	23.77		23.48			0.37			
696	67.6	169.2			20.76						
697	135.8	116.1	21.11	20.20	18.82	0.93	1.44	2.32			

TABLE 4. *Measured redshifts of galaxies in the field of Abell 2390.*

ident. number	redshift	r	B_j-r	rad.vel. km s^{-1}	spec.type visual	S/N	χ^2_{min}	spec.type autom.	telescope	observed lines
108	0.2310 ± 0.0010	20.00	2.16	-48					CFHT	G MgI NaD
155	0.2298 ± 0.0006	19.43	2.08	-340	E	8.8	1.37	E/Sb	WHT+CFHT	G HγHeI MgI FeI
158	0.2370 ± 0.0010	19.53	2.03	1413					CFHT	G MgI NaD
176	0.2120 ± 0.0007	19.69	1.53	-4673	Sd	12.3	1.61	Sc/Sd	WHT	G HγHβMgI
192	0.2347 ± 0.0005	19.42	2.09	853	E	14.0	1.74	E /Sa	WHT+CFHT	G HγHeI HβMgI FeI NaD
211	0.225? ± 0.001	21.42	1.91		E?	3.7	1.93	Sb/Sd?	WHT	MgI
218	1.039? ± 0.001	22.56	0.38		Im?	1.6	1.51	Sb/Im?	"	MgII? OII?
223	0.2339 ± 0.0005	20.19	2.18	658	E	7.2	2.46	E!	"	G HβMgI FeI NaD
236	0.2295 ± 0.0008	20.02	2.31	-413	Sa	4.7	1.46	?	WHT+CFHT	G MgI FeI NaD
239	0.2390 ± 0.0010	20.28	2.16	1900					CFHT	G MgI NaD
240	0.209? ± 0.001	19.25	2.17			2.8	1.54	?	WHT	Hβ?
243	0.23?	22.85*	2.28*		E?	2.4	1.19	?	"	
248	0.2490 ± 0.0010	18.56	2.18	4335					CFHT	G MgI NaD
250	0.214? ± 0.001	21.07	2.02						"	G MgI NaD
255	0.2861 ± 0.0006	19.56	0.87		Sb/Sc	13.9	1.96	Sc	WHT+CFHT	G MgI NaD
273	0.3413 ± 0.0008	19.96	2.14		E	12.1	2.92	E!	WHT	G MgI FeI
275	0.2300 ± 0.0010	18.86	2.45	-291					CFHT	G MgI NaD
286	0.2334 ± 0.0008	18.84	2.39	537	E	7.3	1.66	E/Sa	WHT	G MgI FeI
297	0.2182 ± 0.0007	19.17	2.33	-3164	E	11.0	1.72	E	"	G MgI NaD
299	0.232? ± 0.001	20.35	1.72						CFHT	G MgI NaD
314	0.237? ± 0.001	20.82	2.05			3.8	1.35	?	WHT	MgI?
315	0.2458 ± 0.0004	19.08	1.82	3555	Sb	16.7	6.66	Sb!	WHT+CFHT	K H G HγHeI **HβOIII MgI NI** FeI NaD **OI HαNII SII**
318	0.2516 ± 0.0007	23.17	–	4968	Sa	4.7	1.72	E/Sc?	WHT	G HβMgI NaD
324	0.5209 ± 0.0008	21.08	2.14		Sb	3.9	1.39	?	"	K H G
337	0.2289 ± 0.0006	18.92	2.21	-559	E	17.1	1.56	E	"	G HeI HβMgI FeI Hα
339	0.2310 ± 0.0010	21.09	1.99	-48	E	12.0	1.42	E	WHT+CFHT	G HγHeI HβMgI FeI Hα
341	0.2304 ± 0.0004	17.55	2.02	-194	Sb	15.8	1.72	Sa/Sc	WHT+CFHT	K H G HγHeI **HβOIII MgI NI** FeI NaD **OI HαNII SII**
350	0.2330 ± 0.0010	19.05	2.19	439					CFHT	G MgI NaD
355	0.2261 ± 0.0014	20.87	1.98	-1241	Sa	4.0	1.37	?	WHT	MgI
356	0.2360 ± 0.0008	20.31	2.18	1170	Sa	6.4	1.35	E/Sc	WHT+CFHT	G MgI NaD
359	0.2140 ± 0.0010	23.37	2.15*	-4186	Sa	4.1	1.49	E/Sc?	WHT	MgI
364	0.2334 ± 0.0006	19.13	2.37	537	E	17.0	1.99	E	WHT+CFHT	G HeI HβMgI FeI NaD
365	0.2357 ± 0.0007	20.13	2.27	1097	E	9.4	2.62	E!	WHT+CFHT	G MgI FeI NaD
371	0.3478 ± 0.0014	20.21	1.84		Sa	3.8	1.80	E/Sb?	WHT	MgI
374	0.2311 ± 0.0010	20.36	2.15	-23	E	4.6	2.62	E?!	"	G MgI
388	0.2311 ± 0.0005	18.66	2.26	-23	E	20.5	1.61	E	WHT+CFHT	G HγHeI HβMgI FeI NaD Hα
390	0.2270 ± 0.0010	18.83	2.24	-1022					CFHT	G MgI NaD
391	0.2003 ± 0.0010	21.06	1.04		Im	3.6	1.54	?	WHT	MgI NaD

TABLE 4. *(continued)*

ident. number	redshift	r	B_j-r	rad.vel. km s^{-1}	spec.type visual	S/N	χ^2_{min}	spec.type autom.	telescope	observed lines
396	0.231? ± 0.001	23.85*	0.77*						CFHT	G MgI NaD
413	0.2067 ± 0.0005	20.31	1.61		Sa	14.8	3.42	Sb!	WHT	G HγHeI HβMgI FeI NaD Hα
415	0.194? ± 0.0014	20.68	1.70		E/Sc	3.5	1.54	?	WHT	MgI?
421	0.2386 ± 0.0008	19.85	2.10	1803	E	5.3	1.42	E/Sc	"	G HβMgI
426	0.2118 ± 0.0010	23.10*	–	-4722	E	4.8	1.90	E/Sa?	"	MgI NaD
432	0.2421 ± 0.0005	19.45	2.18	2655	E	14.0	1.54	E	"	G HγHeI HβMgI FeI NaD
435	0.2301 ± 0.0006	19.48	2.29	-267	E	13.1	1.72	E	"	G HeI HβMgI FeI NaD
440	0.2307 ± 0.0006	20.14	2.14	-121	E	6.5	1.32	E/Sb	ESO	K H G HγHeI
452	0.1992 ± 0.0014	22.66	–			1.2	1.23	?	WHT	MgI
454	0.23?	23.26	2.32*		E?	5.1	1.54	E/Sc	"	
461	0.9132 ± 0.0006	21.81	1.69		Sc	2.7	1.42	?	"	**OII** CN K H G
470	0.237? ± 0.001	20.34	2.35						CFHT	G MgI NaD
477	0.23?	20.84	0.92		Im?	3.0	1.06	?	WHT	
486	0.2336 ± 0.0005	19.89	1.62	585	Sb	12.1	1.64	Sa/Sc	"	G **HβOIII** MgI FeI NaD **HαSII**
495	0.2205 ± 0.0005	18.77	2.29	-2604	E	20.1	2.19	E!	"	G HeI HβMgI FeI NaD Hα
498	0.2215 ± 0.0010	20.51	2.32	-2360	Sa/Sc	5.5	1.49	?	"	G NaD
499	0.228? ± 0.001	22.25	2.04			3.6	1.08	?	"	Hβ?
522	0.6276 ± 0.0004	21.33	1.11		Sd	8.7	2.72	Im!	WHT+ESO	MgII **OII** K H G **HγHβ OIII** MgI
530	0.2283 ± 0.0005	19.29	2.32	-705	E	13.6	8.12	E!	WHT	G HγHeI HβMgI FeI NaD Hα
556	0.244? ± 0.001	19.90	2.19						CFHT	
557	0.2190 ± 0.0010	20.57	1.95	-2969	E?	5.8	2.69	E!	WHT+CFHT	MgI NaD
560	0.206? ± 0.001	19.29	1.88		E?	3.5	1.44	E/Sc?	WHT	G HβMgI
570	0.2262 ± 0.0005	18.36	2.27	-1216	E	18.1	10.56	E!	"	G HγHeI HβMgI FeI NaD Hα
588	0.2308 ± 0.0005	18.65	2.24	-96	E	21.2	4.28	E!	"	G HγHeI HβMgI FeI NaD
601	0.23?	19.22	2.13		E?	2.8	1.56	?	"	
602	0.2083 ± 0.0007	18.23	1.46		Sb	17.8	2.79	Sb!	"	G HeI HβMgI
616	0.2381 ± 0.0005	19.57	0.87	1681	Im	10.5	4.71	Im!	ESO	**OII** CN K H G **HγHβOIII**
650	0.3135 ± 0.0010	18.88	2.02		E	15.2	3.84	Sa!	"	K H
657	0.2412 ± 0.0005	20.56	1.82	2436	E	8.8	2.34	Sa!	WHT	**HβOIII** MgI FeI **HαNII**
660	0.23?	21.04	1.56		E?	2.1	1.21	?	"	
665	0.2327 ± 0.0005	19.24	2.37	366	Sa	12.9	1.44	Sa/Sb	ESO	K H G HγHeI HβMgI FeI
692	0.1792 ± 0.0005	18.77	2.04		E	15.9	1.44	E/Sb	"	K H G HγHeI HβMgI FeI
697	0.2312 ± 0.0004	18.82	2.32	1	E	17.0	9.86	E!	WHT+ESO	K H G HγHeI HβMgI FeI NaD
698	0.2236 ± 0.0008	–	–	-1849	E/Sa	7.5	1.54	E/Sc	ESO	K H G

notes : emission lines are in boldface. 341 is the central cD galaxy and 388 the galaxy near the arc. * when r or B_j is not available, R_b or B_b-R_b is given.

identification of lines : MgII : 2799 Å, OII : [OII] 3727 Å, CN : 3883 Å, K : CaII 3934 Å, H : CaII 3968 Å, G : CH 4300 Å, HeI : 4388 Å, Hβ : 4861 Å, OIII : [OIII] 4959 and 5007 Å, MgI : 5175 Å, NI : [NI] 5199 Å, NaD : 5890-5896 Å, FeI : 5270 Å, OI : [OI] 6300 Å, Hα : 6563 Å, NII : [NII] 6583 Å, SII : [SII] 6717-6734 Å

TABLE 5. *Spectroscopically identified stars in the field of Abell 2390.*

ident. number	r	$B_j - r$
173	19.09	1.82
222	20.75	1.05
270	18.91	1.09
348	18.96	2.31
368	17.02	0.79
383	19.85	0.82
389	18.44	0.92
527	18.39	0.99
579	18.47	1.50
589	18.55	2.36
595	20.69	2.22
651	17.74	1.00
699	–	–

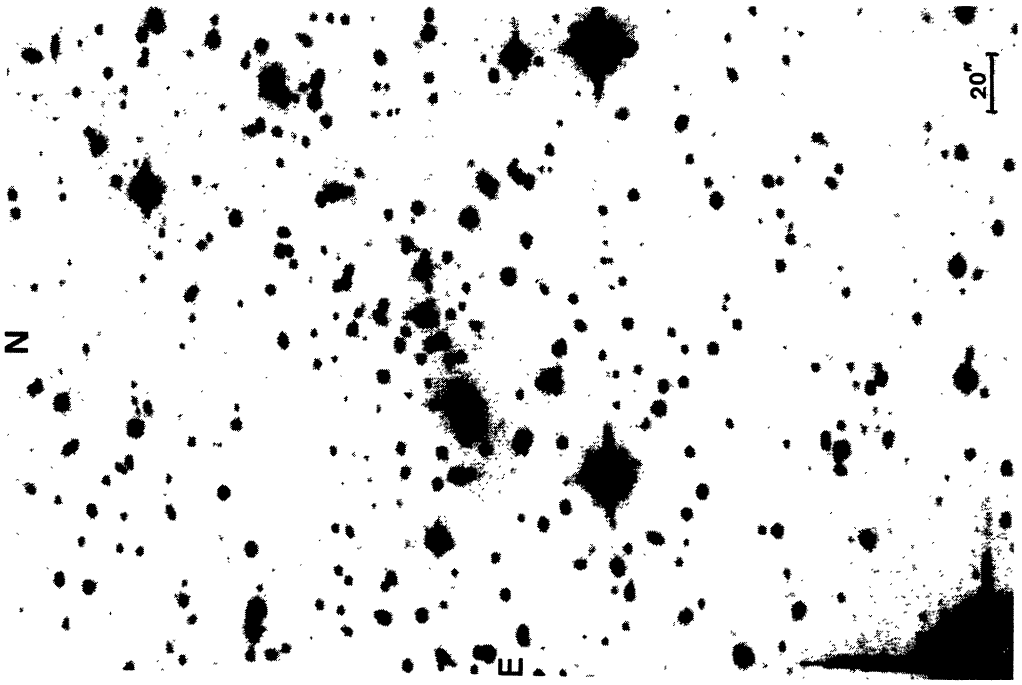

FIGURE 1. *r* CCD frame from INT.

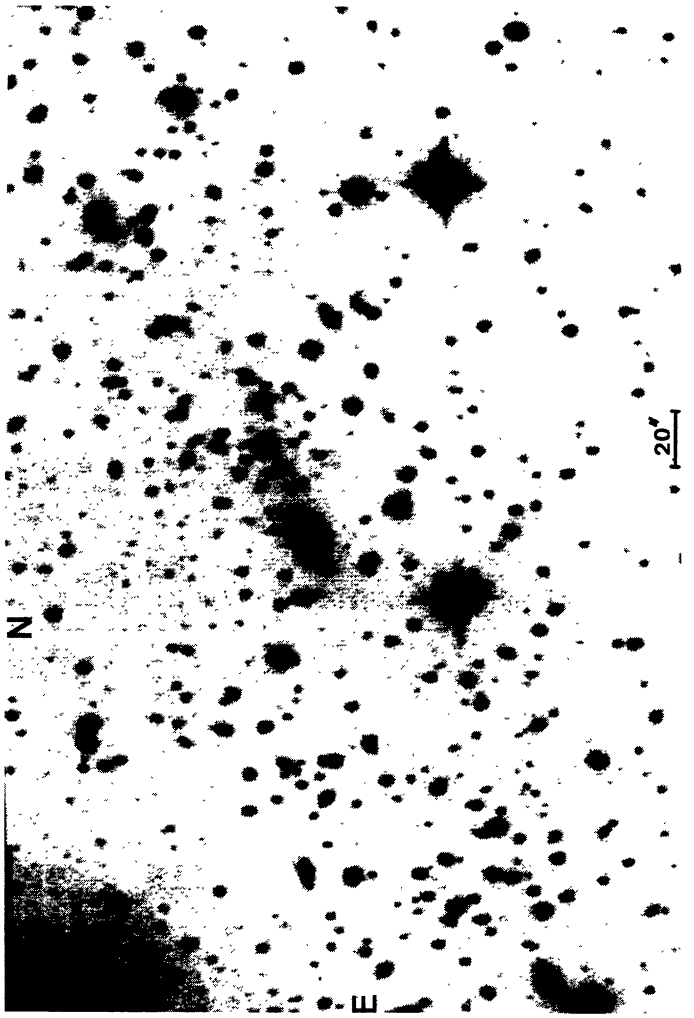

FIGURE 2. Same as Figure 1 rotated by 90°.

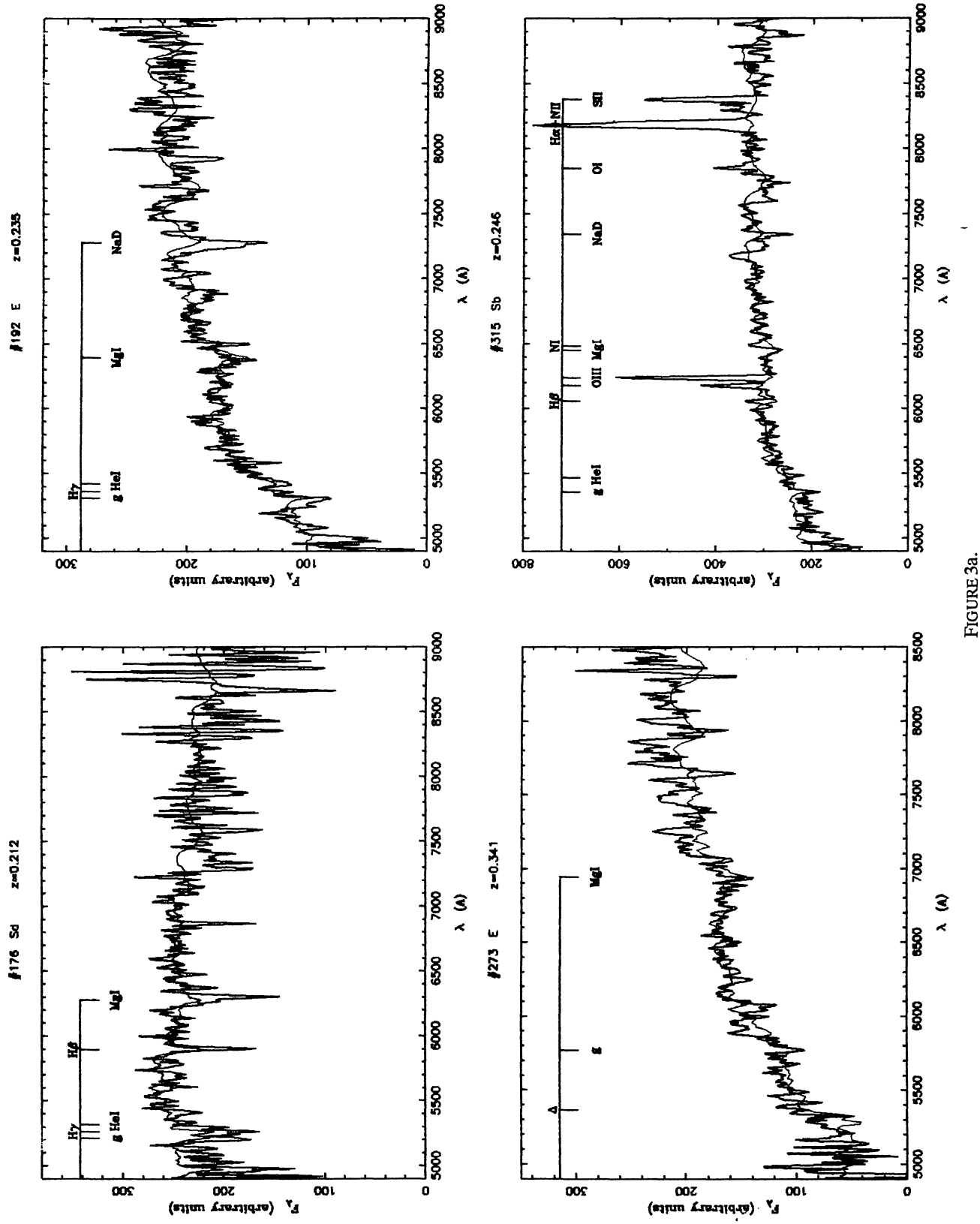

FIGURE 3a.

FIGURE 3. Some spectra obtained with the WHT (Fig. 3a to 3d) and the ESO 3.6m telescope (Fig 3e). A synthetic spectrum from Rocca and Guiderdoni (1988) is also plotted. These synthetic spectra, redshifted to the redshift of the galaxy, are the ones which better fit the observed spectra. The label at the top of each spectrum gives the identification number of the galaxy, the spectral type of the plotted synthetic spectrum and the redshift.

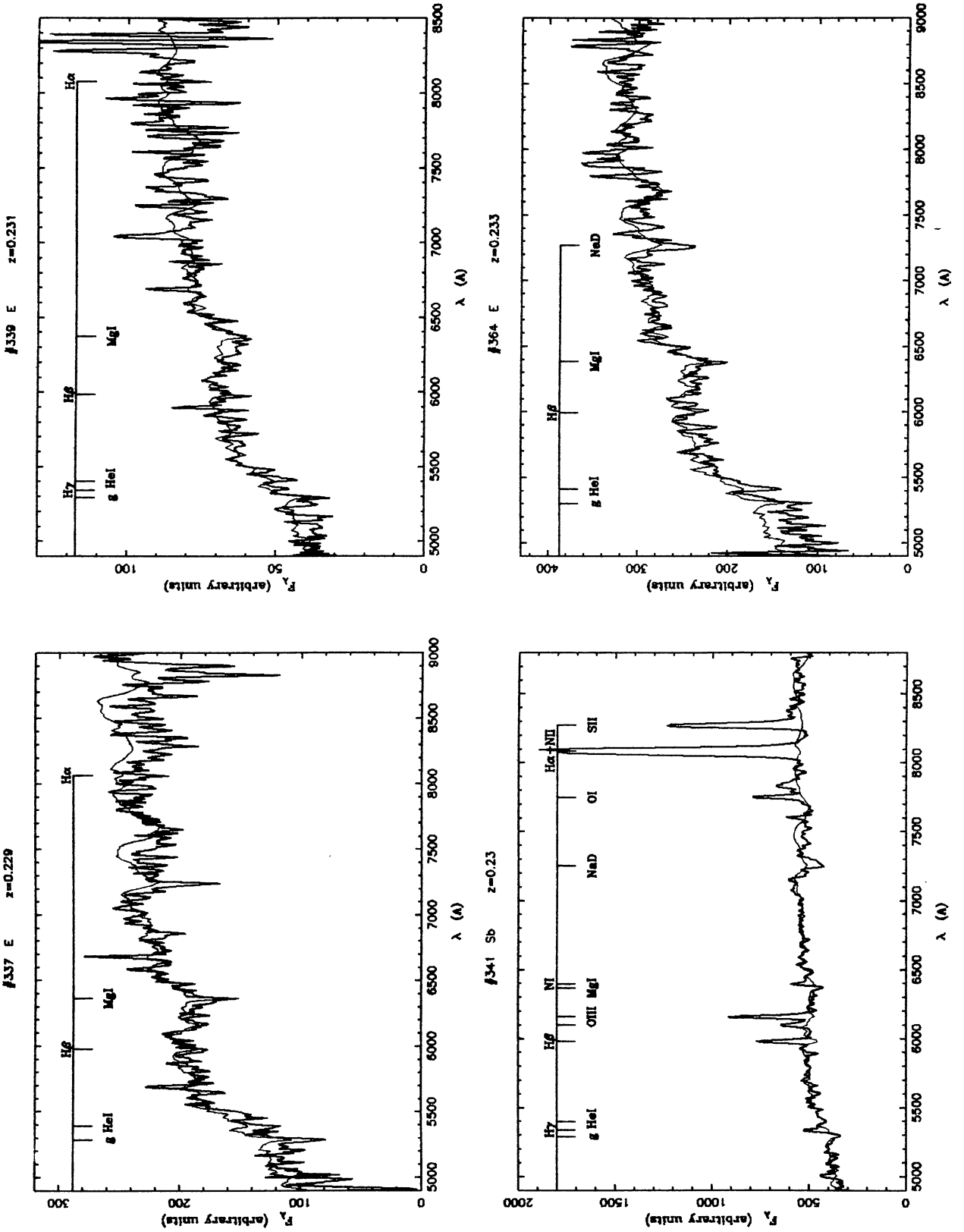

FIGURE 3b.

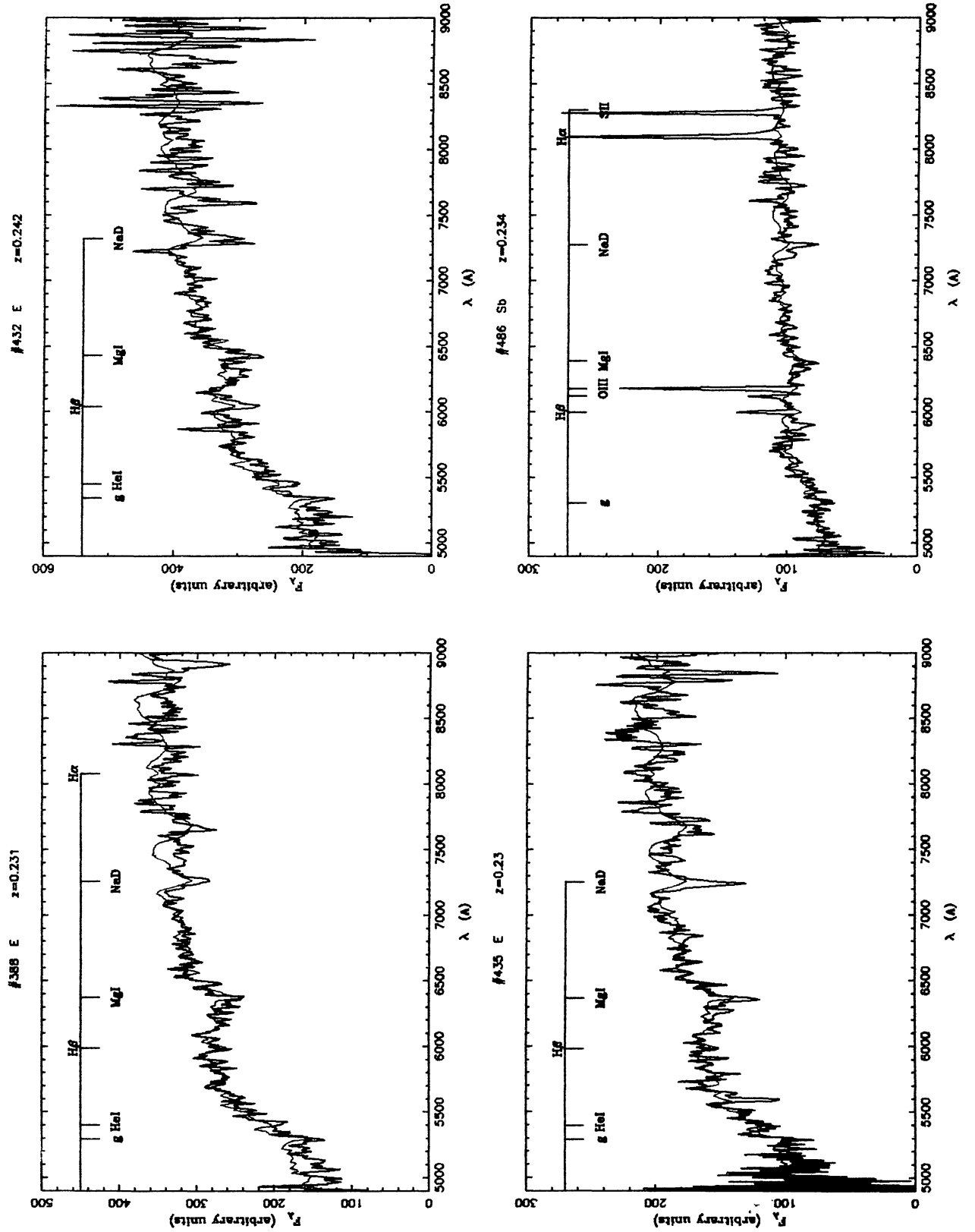

FIGURE 3c.

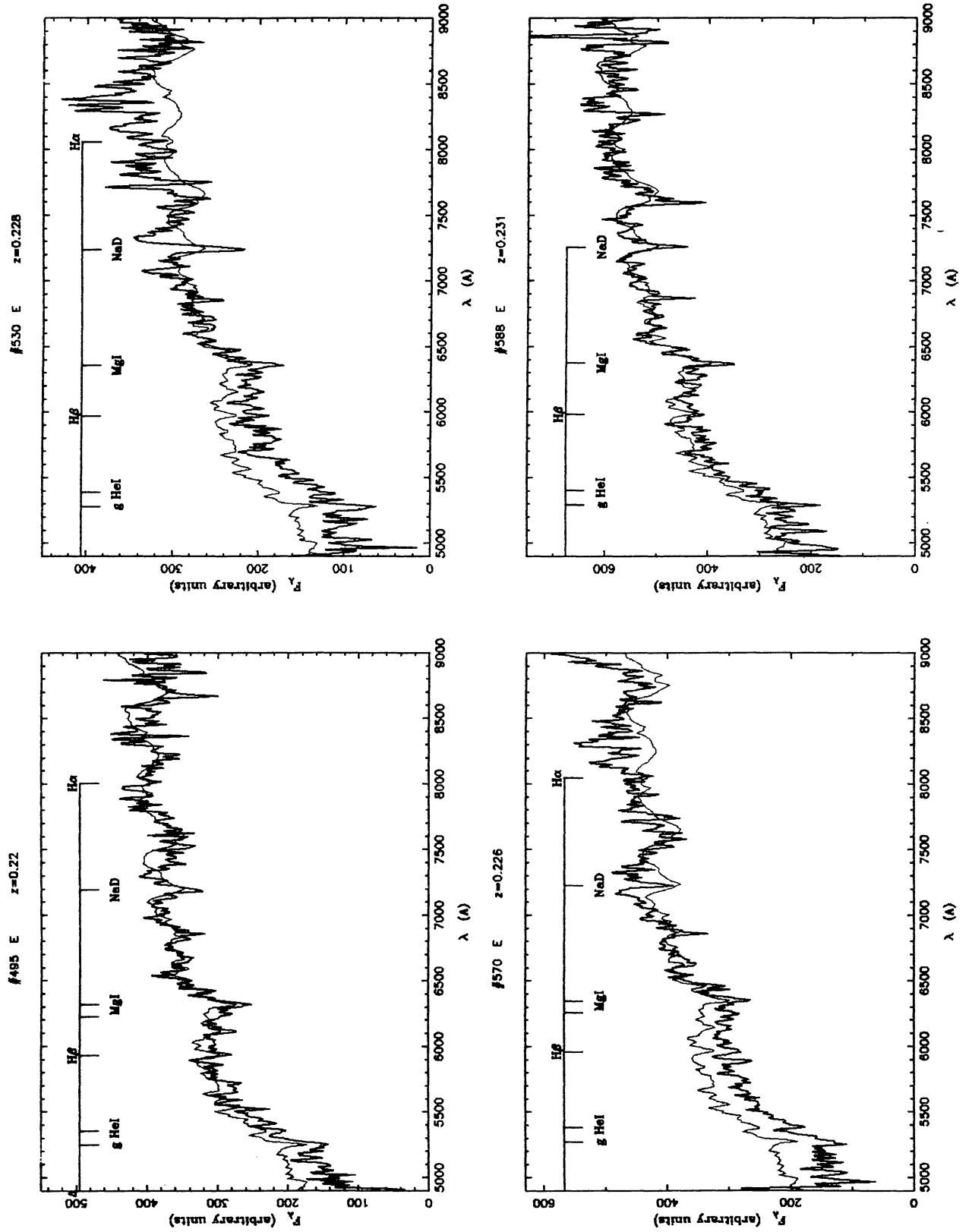

FIGURE 3d.

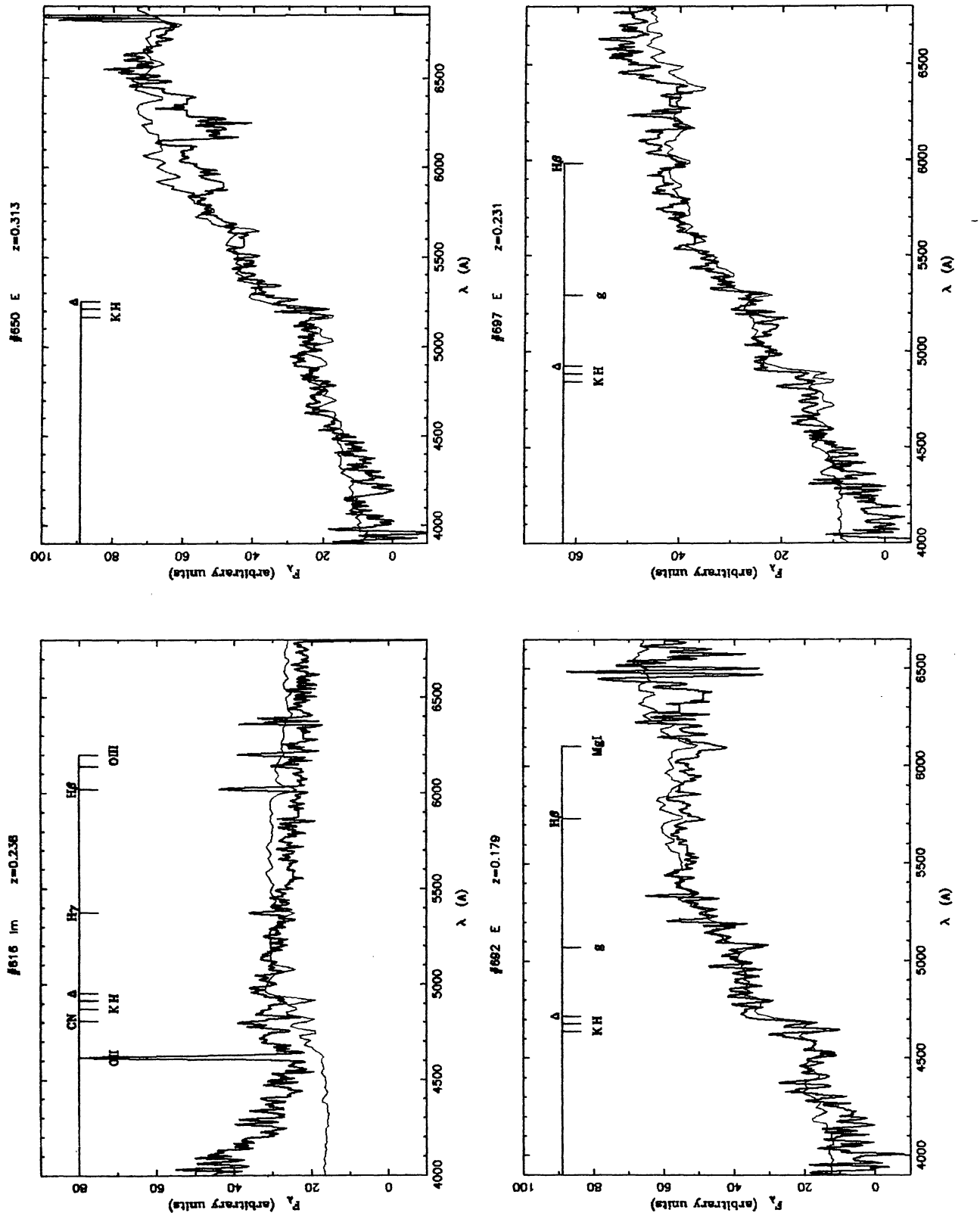

FIGURE 3e.

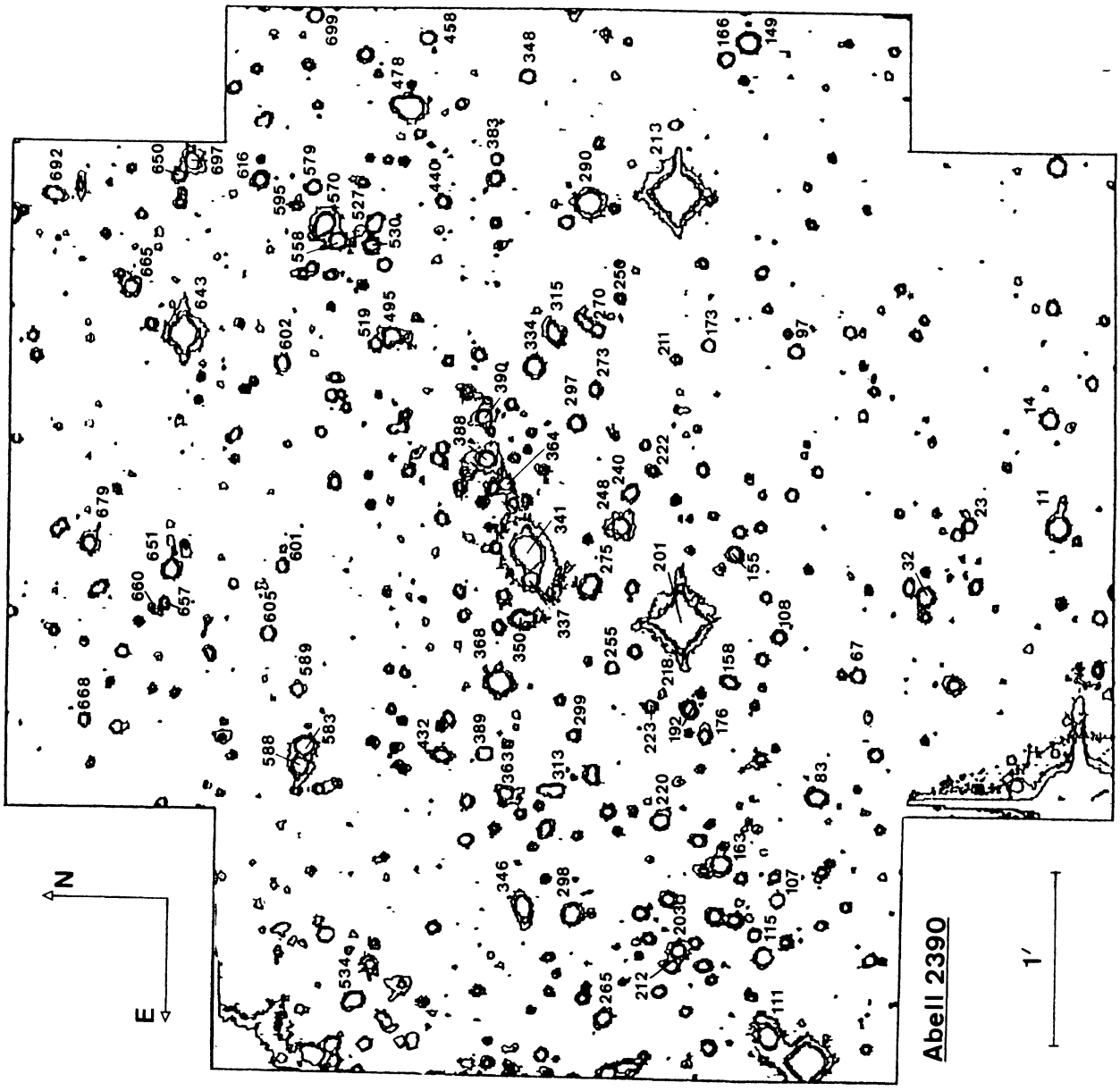

FIGURE 4. 6.3′ × 6.3′ isophotal contour map from *r* INT CCD frames with identification numbers for the brightest objects.

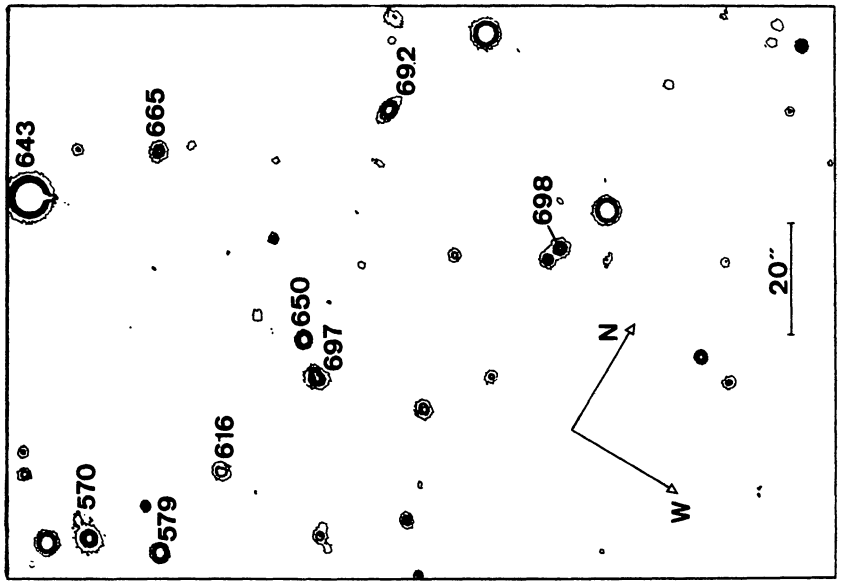

FIGURE 6. 1.7′ × 2.4′ isophotal contour map around object # 698.

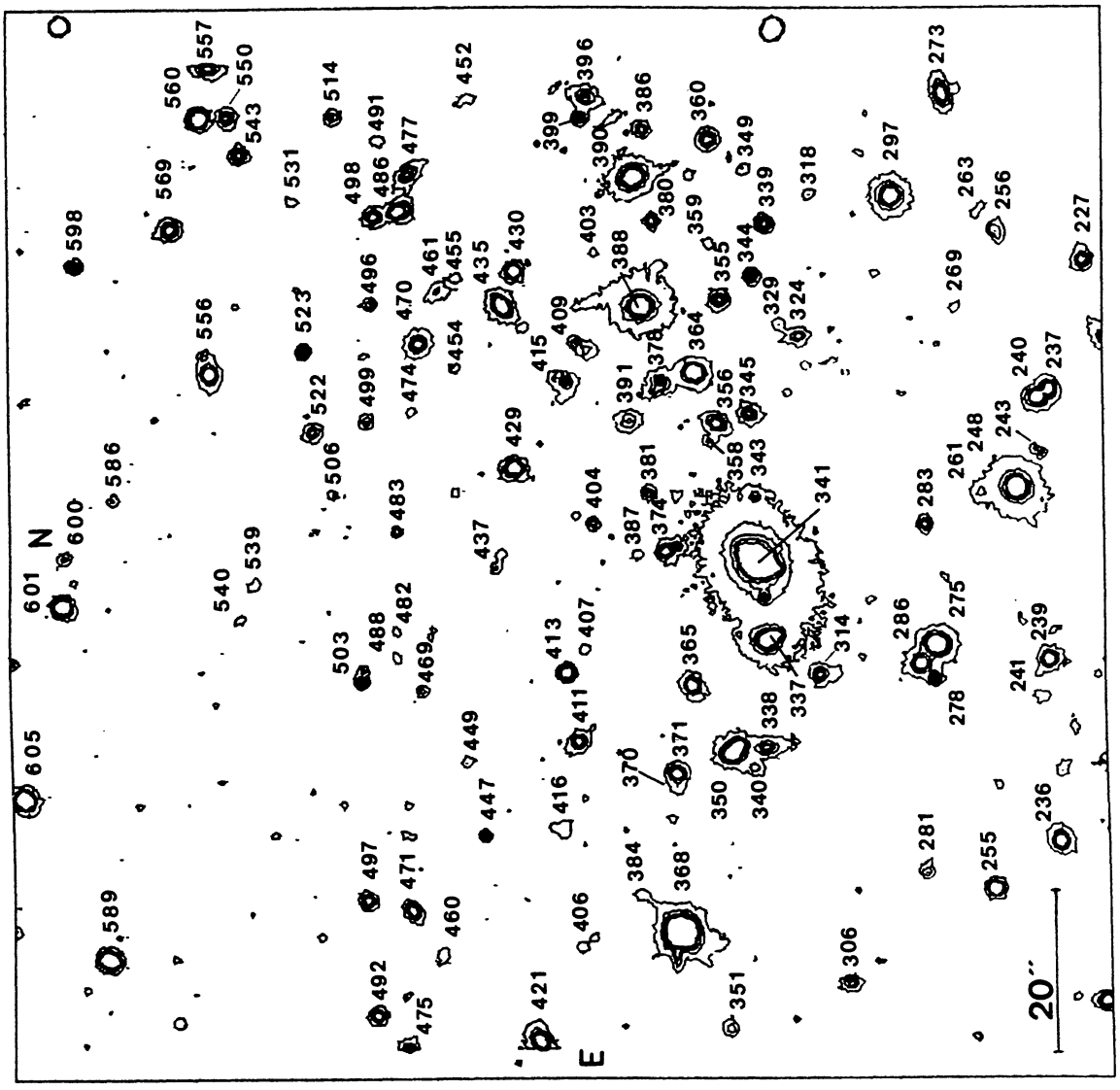

FIGURE 5. 2.2′ × 2.2′ isophotal contour map of the central region from *R* CFHT CCD frames with identification numbers.